samples. RNA from the tissues were prepared using the RecoverAll Total RNA Isolation Kit (Ambion). The isolated RNA was subjected to qRT-PCR for miR-16 as described above.

MiR-16 functional pathway analysis. For preparation of RNA samples, PC-3M-luc cells were reverse transfected in quadruplicate by complexing miR-16 and NC miRNA and NeoFX transfection reagent (Ambion). The final concentration of miRNA was 30 nmol/l. Cells were harvested at 72 hours post-transfection. One microgram of total RNA per sample was used to prepare biotin-labeled cRNA using a MessageAmp II-based protocol (Ambion) and one round of amplification. Labeled cRNA was hybridized, washed, and scanned using Illumina's recommended protocols. Illumina BeadScan software was used to produce .idat, .xml, and .tif files for each array on a slide. Raw data were extracted using Illumina BeadStudio software, v 3.0 (Illumina, San Diego, CA). Following quality assessment, data from the replicate beads on each array were summarized into average intensity values and variances. The background subtracted data were used to compare the relative expression of mRNAs in cells transfected with miR-16, NC miRNA, and transfection agent only. analysis of variance was used to judge the significance of the variation observed between the various treatment groups. In total, 285 mRNAs exceeded the thresholds used to identify differentially expressed genes (log ratio greater than 0.5 or less than −0.5 for the average signal between miR-16 and NC miRNA or transfection agent only treatments and P values <0.001 for the 72 hour time-point).

Statistical analysis. The results are given as mean ± SD Statistical analysis was conducted using the analysis of variance with the Bonferroni correction for multiple comparisons. A P value of ≤0.05 was considered to indicate a significant difference.

SUPPLEMENTARY MATERIAL

Figure S1. The scheme of dual luciferase assay for monitoring of systemic miR-16 delivery.

Figure S2. Overview of experimental protocol for inhibition of metastatic tumor growth in bone tissues by the atelocollagen-mediated miRNA treatment.

Figure S3. KEGG cell cycle diagram.

Table S1. Data of the mRNA array for comparison of miR-16 and NC miR transfected PC-3M-luc cells.

ACKNOWLEDGMENTS

We thank Ayako Inoue, Ayano Matsumoto, and Maho Kodama for their excellent technical work. We also thank Shunji Nagahara of Formulation Research Laboratories, Technology Research and Development Center, Dainippon Sumitomo Pharma Co., Ltd. for technological support and Koken Co., Ltd. for providing atelocollagen. This work was supported in part by a Grant-in-Aid for the Third-Term Comprehensive 10-Year Strategy for Cancer Control, a Grant-in-Aid for Scientific Research on Priority Areas Cancer from the Ministry of Education, Culture, Sports, Science and Technology, and the Program for Promotion of Fundamental Studies in Health Sciences of the National Institute of Biomedical Innovation (NiBio), and a Takeda Science Foundation.

REFERENCES

1. Calin, GA, Sevignani, C, Dumitru, CD, Hyslop, T, Noch, E, Yendamuri, S *et al.* (2004). Human microRNA genes are frequently located at fragile sites and genomic regions involved in cancers. *Proc Natl Acad Sci USA* **101**: 2999–3004.
2. Calin, GA, Ferracin, M, Cimmino, A, Di Leva, G, Shimizu, M, Wojcik, SE *et al.* (2005). A microRNA signature associated with prognosis and progression in chronic lymphocytic leukemia. *N Engl J Med* **353**: 1793–1801.
3. Calin, GA and Croce, CM (2006). MicroRNA-cancer connection: the beginning of a new tale. *Cancer Res* **66**: 7390–7394.
4. Lu, J, Getz, G, Miska, EA, Alvarez-Saavedra, E, Lamb, J, Peck, D *et al.* (2005). MicroRNA expression profiles classify human cancers. *Nature* **435**: 834–838.
5. Volinia, S, Calin, GA, Liu, CG, Ambs, S, Cimmino, A, Petrocca, F *et al.* (2006). A microRNA expression signature of human solid tumors defines cancer gene targets. *Proc Natl Acad Sci USA* **103**: 2257–2261.
6. Mattie, MD, Benz, CC, Bowers, J, Sensinger, K, Wong, L, Scott, GK *et al.* (2006). Optimized high-throughput microRNA expression profiling provides novel biomarker assessment of clinical prostate and breast cancer biopsies. *Mol Cancer* **5**: 24.
7. Porkka, KP, Pfeiffer, MJ, Waltering, KK, Vessella, RL, Tammela, TL and Visakorpi, T (2007). MicroRNA expression profiling in prostate cancer. *Cancer Res* **67**: 6130–6135.
8. Bonci, D, Coppola, V, Musumeci, M, Addario, A, Giuffrida, R, Memeo, L *et al.* (2008). The miR-15a-miR-16-1 cluster controls prostate cancer by targeting multiple oncogenic activities. *Nat Med* **14**: 1271–1277.
9. Bullrich, F and Croce, CM (2001). Molecular biology of chronic lymphocytic leukemia. In: Cheson, B (ed.). *Chronic Lymphoid Leukemia*. Dekker: New York, pp. 9–32.
10. Dong, JT, Boyd, JC and Frierson, HF (2001). Loss of heterozygosity at 13q14 and 13q21 in high grade, high stage prostate cancer. *Prostate* **49**: 166–171.
11. Calin, GA, Dumitru, CD, Shimizu, M, Bichi, R, Zupo, S, Noch, E *et al.* (2002). Frequent deletions and down-regulation of micro-RNA genes miR15 and miR16 at 13q14 in chronic lymphocytic leukemia. *Proc Natl Acad Sci USA* **99**: 15524–15529.
12. Calin, GA and Croce, CM (2006). Genomics of chronic lymphocytic leukemia microRNAs as new players with clinical significance. *Semin Oncol* **33**: 167–173.
13. Takeshita, F, Minakuchi, Y, Nagahara, S, Honma, K, Sasaki, H, Hirai, K *et al.* (2005). Efficient delivery of small interfering RNA to bone-metastatic tumors by using atelocollagen *in vivo*. *Proc Natl Acad Sci USA* **102**: 12177–12182.
14. Yin, Z, Spitz, MR, Babaian, RJ, Strom, SS, Troncoso, P and Kagan, J (1999). Limiting the location of a putative human prostate cancer tumor suppressor gene at chromosome 13q14.3. *Oncogene* **18**: 7576–7583.
15. Arguello, F, Furlanetto, RW, Baggs, RB, Graves, BT, Harwell, SE, Cohen, HJ *et al.* (1992). Incidence and distribution of experimental metastases in mutant mice with defective organ microenvironments (genotypes Sl/Sld and W/Wv). *Cancer Res* **52**: 2304–2309.
16. Jenkins, DE, Yu, SF, Hornig, YS, Purchio, T and Contag, PR (2003). *In vivo* monitoring of tumor relapse and metastasis using bioluminescent PC-3M-luc-C6 cells in murine models of human prostate cancer. *Clin Exp Metastasis* **20**: 745–756.
17. Cimmino, A, Calin, GA, Fabbri, M, Iorio, MV, Ferracin, M, Shimizu, M *et al.* (2005). miR-15 and miR-16 induce apoptosis by targeting BCL2. *Proc Natl Acad Sci USA* **102**: 13944–13949.
18. Johnson, CD, Esquela-Kerscher, A, Stefani, G, Byrom, M, Kelnar, K, Ovcharenko, D *et al.* (2007). The let-7 microRNA represses cell proliferation pathways in human cells. *Cancer Res* **67**: 7713–7722.
19. Kanehisa, M, Araki, M, Goto, S, Hattori, M, Hirakawa, M, Itoh, M *et al.* (2008). KEGG for linking genomes to life and the environment. *Nucleic Acids Res* **36**(Database issue): D480–D484.
20. Kanehisa, M and Goto, S (2000). KEGG: Kyoto Encyclopedia of Genes and Genomes. *Nucleic Acids Res* **28**: 27–30.
21. Kanehisa, M, Goto, S, Hattori, M, Aoki-Kinoshita, KF, Itoh, M, Kawashima, S *et al.* (2006). From genomics to chemical genomics: new developments in KEGG. *Nucleic Acids Res* **34**(Database issue): D354–D357.
22. Dennis, G, Sherman, BT, Hosack, DA, Yang, J, Gao, W, Lane, HC *et al.* (2003). DAVID: Database for Annotation, Visualization, and Integrated Discovery. *Genome Biol* **4**: P3.
23. Lu, W, Takahashi, H, Furusato, M, Maekawa, S, Nakano, M, Meng, C *et al.* (2006). Allelotyping analysis at chromosome 13q of high-grade prostatic intraepithelial neoplasia and clinically insignificant and significant prostate cancers. *Prostate* **66**: 405–412.
24. Chan, JA, Krichevsky, AM and Kosik, KS (2005). MicroRNA-21 is an antiapoptotic factor in human glioblastoma cells. *Cancer Res* **65**: 6029–6033.
25. Cheng, AM, Byrom, MW, Shelton, J and Ford, LP (2005). Antisense inhibition of human miRNAs and indications for an involvement of miRNA in cell growth and apoptosis. *Nucleic Acids Res* **33**: 1290–1297.
26. Johnson, SM, Grosshans, H, Shingara, J, Byrom, M, Jarvis, R, Cheng, A *et al.* (2005). RAS is regulated by the let-7 microRNA family. *Cell* **120**: 635–647.
27. Lim, LP, Lau, NC, Garrett-Engele, P, Grimson, A, Schelter, JM, Castle, J *et al.* (2005). Microarray analysis shows that some microRNAs downregulate large numbers of target mRNAs. *Nature* **433**: 769–773.
28. Lewis, BP, Burge, CB and Bartel, DP (2005). Conserved seed pairing, often flanked by adenosines, indicates that thousands of human genes are microRNA targets. *Cell* **120**: 15–20.
29. Ovcharenko, D, Jarvis, R, Hunicke-Smith, S, Kelnar, K and Brown, D (2005). High-throughput RNAi screening *in vitro*: from cell lines to primary cells. *RNA* **11**: 985–993.
30. Weil, D, Garçon, L, Harper, M, Duménil, D, Dautry, F and Kress, M (2002). Targeting the kinesin Eg5 to monitor siRNA transfection in mammalian cells. *BioTechniques* **33**: 1244–1248.

Cancer Gene Therapy (2009), 1–10
 0929-1903/09 $32.00
www.nature.com/cgt

ORIGINAL ARTICLE

Mutant mouse *p53* transgene elevates the chemical induction of tumors that respond to gene silencing with siRNA

H Tanooka[1], K Tatsumi[1], H Tsuji[1], Y Noda[1], T Katsube[1], H Ishii[1], A Ootsuyama[2], F Takeshita[3] and T Ochiya[3]

[1]*Biological Effects Research Group, Research Center for Radiation Protection, National Institute of Radiological Sciences, Chiba, Japan;* [2]*Department of Radiation Biology and Health, University of Occupational and Environmental Health, Kita-Kyushu, Japan and* [3]*Section for Studies on Metastasis, National Cancer Center Research Institute, Tokyo, Japan*

To study the role of mutant *p53* in the induction and cure of tumors, we generated transgenic mice carrying mutant *p53* (m*p53*) containing a 9 bp deletion in exon 6 in addition to wild-type *p53*, expressing both *p53* and m*p53*. The m*p53* cDNA was cloned from a radiation-induced mouse tumor and ligated to the chicken β-actin promoter/CMV-IE enhancer in the expression vector. The presence of m*p53* suppressed *p21* expression in primary fibroblasts after ionizing irradiation, indicating the dominant-negative activity of m*p53* in the mice. These mice developed fibrosarcomas after the subcutaneous injection of 3-methylcholanthrene with an incidence 1.7-fold higher than that of wild-type mice (42% excess). The tumors were then treated via a potent atelocollagen delivery system with small interfering RNA (siRNA), that targeted the promoter/enhancer of the expression vector, resulting in the suppression of tumor growth in 30% of 44 autochthonous tumors, including four cures, and their transplants, the total fraction corresponding to the tumor excess. This suppressive effect involved the induction of apoptosis. These results indicate that m*p53* activity causes tumors that can be suppressed by subsequent silencing of m*p53* in the presence of wild-type *p53* alleles.
Cancer Gene Therapy advance online publication, 26 June 2009; doi:10.1038/cgt.2009.43

Keywords: mutant *p53*; transgenic mice; tumor; siRNA gene silencing; apoptosis

Introduction

The *p53* gene is a tumor suppressor, controlling the cell cycle and apoptosis,[1,2] protecting the irradiated mouse fetus from teratogenesis[3] and regulating mouse reproduction.[4] Mutated *p53* is frequently found in human cancers.[5] and predisposes Li–Fraumeni syndrome patients to cancer.[6]

Heterozygous mice with various *p53* mutations have been used to study the effects of these mutations on tumor induction. Mice carrying *p53* mutated at codon135 are highly sensitive to spontaneous[7,8] and chemical tumor induction.[9] Mice carrying *p53* mutations analogous to the human Li–Fraumeni syndrome hot spot mutation exhibit a high incidence of spontaneous tumors with a spectrum different from that of *p53*-null mice,[10–12] a high metastatic potential for produced tumors[13] and a high incidence of chemically induced tumors.[14] Especially of note is an approach toward simulating the human context with heterozygous mice containing human *p53* and Li–Fraumeni mutant *p53* in the genome.[12]

At the initial step of carcinogenesis caused by p53 mutation, there must exist a heterozygous state of wild-type *p53* with mutant *p53*, resulting in the expression of both types of p53 proteins. Mutant p53 proteins act in a dominant-negative manner by interfering with the activity of wild-type p53 proteins, thus exerting gain-of-function activity.[12,15,16] This activity induces tumor formation by interfering with the *ATM*-controlled molecular network protecting cells from tumorigenesis. A recent study reported that mutant p53 interferes with the binding of the repair protein complex, Mre11-Rad50-NBS1, to radiation-induced DNA double strand breaks,[12] suggesting an additional role of mutant *p53* in DNA repair and tumorigenesis.

On the other hand, the absence of *p53* expression in mice results in a high incidence of tumors.[17,18] By restoring wild-type *p53* function via Cre recombinase-mediated reactivation, such tumors regress after apoptosis[19] or cellular senescence.[20] However, such restoration may not function in the presence of mutant p53 protein because of its dominant-negative action over the

Correspondence: Dr H Tanooka, Biological Effects Research Group, Research Center for Radiation Protection, National Institute of Radiological Sciences, 4-9-1 Anagawa, Inage-ku, Chiba 263-8555, Japan.
E-mail: tanooka-h@wind.ocn.ne.jp; tnk@nirs.go.jp
Received 3 August 2008; revised 3 February 2009; accepted 22 March 2009

wild-type. The remaining wild-type *p53* allele is often lost in the tumors of *p53*-heterozygous hosts[6]; therefore, curing tumors by restoring wild-type *p53* activity cannot be expected.

Curing autochthonous tumors in experimental animals induced either spontaneously, chemically or with radiation, is an essential approach to achieving a true cure for cancer.[21] Mouse fibrosarcomas induced by 3-methylcholanthrene (MCA) are a suitable model for experimental therapy, because of their well-characterized growth kinetics.[22] Curing autochthonous MCA-induced tumors with ionizing radiation is very difficult; after temporary regression, most regrow with the same clonal nature of the primary tumor, whereas transplanted tumors of the same origin are easily cured with 44 Gy of the dose needed to cure 50% of tumors.[23,24] This discrepancy may be explained by the differences in adaptive immunity between autochthonous and transplanted tumor environments.[25] Therefore, our final targets for cure experiments are autochthonous tumors.

Gene silencing by RNA interference is a promising approach for suppressing tumors.[26] In our transgenic mice, mutant *p53* cDNA was introduced in addition to intact wild-type *p53* alleles; thus the loss of the wild-type *p53* allele frequently observed in the tumors of mutant *p53*-heterozygous mice is unlikely to occur. Using this advantage, we attempted to silence only the mutant *p53* transgene, not wild-type *p53,* using siRNA designed to target the promoter/enhancer of the transgene. If the mutant *p53* causes the tumors, it should respond to silencing to an appreciable extent and consequently regress or stop growing.

The effective silencing of transcription by targeting a promoter with siRNA has been shown in cultured human cells to involve DNA methylation of the targeted sequence[27] and the interference of the formation of the transcription–initiation complex with Argonaute proteins leading to heterochromatin formation.[28] In this study, we used siRNA designed to suppress the promoter/enhancer of the mutant *p53* transgene. Atelocollagen, an end-cut collagen, was used as a delivery system to protect siRNA from RNase and introduce siRNA efficiently to the target molecules in the tumor tissue.[29,30]

We report here the construction of transgenic mice carrying intact wild-type *p53* and mutant *p53* cDNA, being homozygous for the wild-type *p53* allele and hemizygous for mutant *p53* ($p53^{+/+;\,m}$). For the sake of convenience, we refer to the $p53^{+/+;\,m}$ mice as m*p53* mice. The presence of mutant *p53* elevated tumor incidence in the presence of intact wild-type *p53* alleles, and these tumors could be suppressed by silencing the mutant *p53* transgene through the reactivation of apoptotic activity.

Materials and methods

Cloning of mutant p53 *cDNA and construction of pTE50*

The original tumor carrying the mutant *p53* was squamous cell carcinoma, chosen from mouse skin tumors with various *p53* mutations generated by repeated β-irradiation.[31] Mutant *p53* cDNA with a 9 bp deletion from codon 191–193 in exon 6 of the *p53* gene, corresponding to the DNA-binding domain of p53, was prepared from the tumor.[32] The *Xho*I/*Kpn*I fragment of the mutant *p53* cDNA, which included the deletion, was first cloned into pBR322, then this fragment was exchanged with the corresponding fragment of the mouse *p53* cDNA clone (RDB1284; Riken, Tsukuba, Japan) containing the exon 2–11 reading frame. The mutant *p53* cDNA fragment cut by *Hind*III/*Xho*I was then inserted downstream of the chicken β-actin gene promoter combined with the CMV-IE enhancer in the 5.8 kb expression vector pCXN2[33] to construct pTE50 (Figure 1a). The DNA nucleotide sequence was determined using Big Dye Terminator v3.1 and ABI Prism 310 analyzer (Applied Biosystems, Warrington, WA) with *p53* primers[32] according to the manufacturer's protocol. The expression of mp53 proteins was confirmed in cultured HEK293 cells harboring pTE50 (Supplementary Figure 1).

Transgenic mice

The *Bam*HI and *Pvu*I digests of pTE50 containing m*p53* cDNA were introduced into the early-stage embryos of C57BL/6J-Jcl mice (Oriental Yeast, Tokyo, Japan). Out of 105 candidate mice from 569 transplanted embryos, 2 transgenic mice, 1 male and 1 female, with mutant *p53* were obtained. The male m*p53* mouse was mated to wild-type C57BL/6J female mice to yield transgenic m*p53* offspring. Mice were maintained according to the National Institute of Radiological Sciences guidelines for animal care. The mice were registered as C57BL/6J-Tg(pTE50)Nrs and frozen embryos were preserved at Riken BioResource Center (Riken).

Southern blot analysis and PCR genotyping of mouse DNA

The DNA was extracted from m*p53* mouse tails using phenol/chloroform after proteinase K (Invitrogen, Carlsbad, CA) digestion at 50 °C overnight, followed by ethanol precipitation. To confirm the presence of m*p53*, the DNA was subjected to Southern blot analysis with vector probe p1 after digestion with *Hind*III (Figure 1b). For genotyping, 1 μl of 100-fold diluted cell lysates was directly applied to PCR in a 20 μl reaction mixture (Ex Taq; Takara Bio, Tokyo, Japan). The PCR reactions were performed in a thermal cycler (Gene Amp 9700; Applied Biosystems, Foster City, CA) for 30 cycles of 94 °C for 30 s, 55 °C for 30 s and 72 °C for 30 s. The PCR products were analyzed by 1% agarose gel electrophoresis.

mRNA-selective PCR

The mRNA-selective PCR utilized deoxyribonucleotide triphosphate analogs as precursors with low annealing and low denaturation temperatures to avoid the amplification of contaminating genomic DNA while synthesizing cDNA.[34] Total RNA was extracted from tissue using Qiagen MiniPrep kit (Qiagen, Hilden, Germany) and 0.35 μg was reverse transcribed to cDNA in a 25 μl

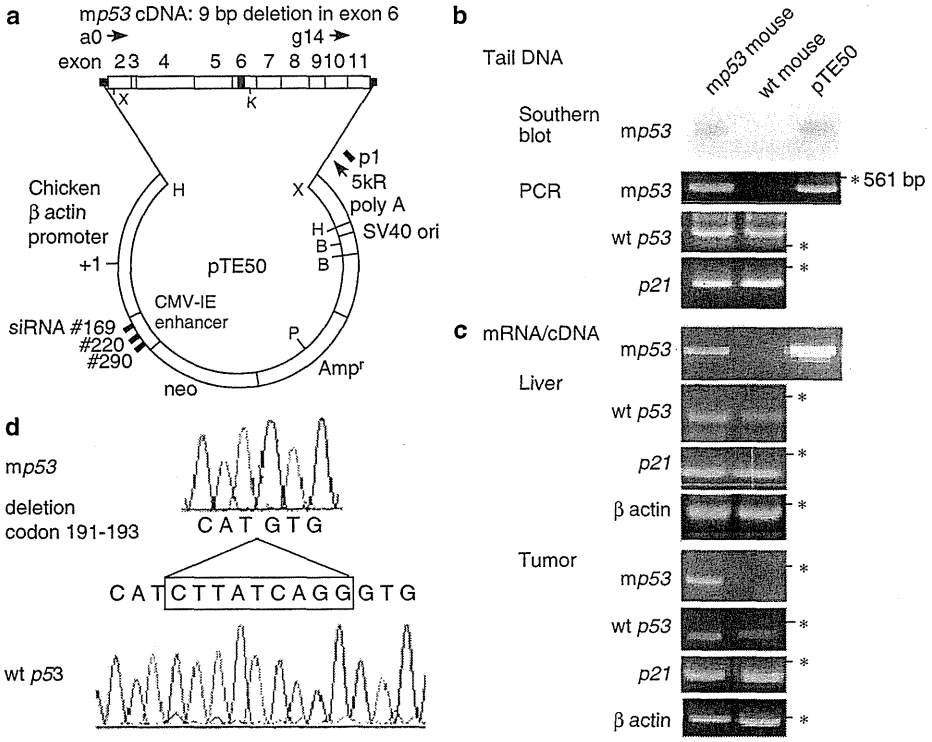

Figure 1 Construction of the plasmid pTE50 with mutant *p53* cDNA and its introduction into the mouse genome. (**a**) Mutant *p53* cDNA containing a 9 bp deletion in exon 6 (1.41 kb) was inserted into expression vector pCXN2 (5.8 kb). Arrows g14 and 5KR indicate PCR primers for genotyping and mRNA-selective PCR. p1: a Southern blot probe. Restriction sites: B, *Bam*HI; H, *Hind*III; K, *Kpn*I; P, *Pvu*I; X, *Xho*I. pTE50 cut with *Bam*HI and *Pvu*I (5.4 kb) was introduced into the mouse genome. (**b**) Representative blot and gels for mouse tail DNA. *Hind*III-cut genomic DNA was electrophoresed and hybridized with probe p1. *Hind*III-cut pTE50 was used as a position marker for Southern blot. PCR primer pairs: g14 and 5kR for the detection of exon 10–11 m*p53*, b1 and I5-3′ for exon 4–intron 5 wild-type *p53*, and B and BR for *p21*. (**c**) mRNA-selective PCR profiles for liver tissues and tumors from m*p53* and wild-type mice. Primer pairs: a0 and 5KR for exon 2–11 m*p53* in the liver (1166 bp) and g14 and 5KR for exon 10–11 m*p53* in the tumor; b1 and 49R for exon 4–6 wild-type *p53*, B and BR for *p21*, and F4 and R2 for mouse β-actin. (**d**) Electropherograms showing the 9 bp deletion from codon 191 to codon 193 in exon 6 in the cDNA of the liver of m*p53* mice (upper) and its presence in the cDNA of the wild-type mouse liver (lower). cDNAs for sequencing were amplified by PCR with primer sets a0 and 5KR for m*p53*, and ex1 and ex11R for wild-type *p53*.

reaction mixture (Takara Bio). A portion of 3 μl of the cDNA reaction was used for mRNA-selective PCR (Takara Bio) in a 20 μl reaction mixture for 25 cycles at 85 °C for 1 min, 45 °C for 1 min and 72 °C for 1 min. The absence of contaminating genomic DNA amplification was confirmed by the absence of the intron-containing PCR products, based on lengths. The dose responses of the mRNA-selective PCR band density to various amounts of total RNA initially added were obtained for m*p53*, *p21* and β-actin (Supplementary Figure 2), and the quantitative range was used to observe the effect of siRNA on m*p53* mRNA expression.

PCR primers

The PCR primers used were the *p53* exon 10 primer g14, 5′-AGGATGCCCATGCTACAGAG-3′ and the vector primer 5KR, 5′-AGCCAGAAGTCAGATGCTCA-3′ to detect the genomic m*p53* and its cDNA; the exon 2 primer a0, 5′-ATGACTGCCATGGAGTCACA-3′ in combination with 5KR to detect the full length of the exon 2–11 reading frame of m*p53* cDNA; b1 in exon 4, 5′-CCATCACCTCACTGCATGGA-3′ and 49R spanning the 9 bp deletion in exon 6, 5′-TTCCACCCTGATAAG ATGCTG-3′ to detect wild-type *p53* cDNA; I5-3′ in intron 5, 5′-GGAATTCCTAAGAGCAAGAATAAGT CAGAA-3′ in combination with b1 to detect genomic wild-type *p53*; ex1 in the 3′ end of exon 1, 5′-CAGGC TTCTCCGAAGACTGG-3′ and ex11hR, 5′-CTGAAG TCATAAGACAGCAA-3′ to detect the full length of exon 2-exon 11 of wild-type *p53* cDNA. Other *p53* primers for sequencing are described elsewhere.[32] Primers to detect *p21* cDNA were B, 5′-TAAAGGGCATCCT GAGCTACACT-3′ and BR, 5′-TTACTCCTTCGAGGC CATGTAGG-3′; and primers to detect mouse β-actin cDNA were F4, 5′-CTAGACTTCGAGCAGGAGAT GG-3′ and R2, 5′-CAGAACAGTCCGCCTAGAAGC-3′.

Analysis of p21 protein in irradiated fetal mouse cells

Embryonic fibroblasts from transgenic and wild-type mice were cultured separately in Dulbecco's modified

Eagle's medium (Sigma, St Louis, MO) supplemented with 10% fetal bovine serum (Calbiochem/Merck, Darmstadt, Germany) and 60 μg ml^{-1} kanamycin in a humidified CO_2 incubator at 37 °C. Cells were seeded at a density of 2.9×10^5 cells in a 9 cm diameter culture dish, grown to a late log growth phase, irradiated by a 200 KVp X-ray generator (Shimazu PANTAK, Model M251-0468, Kyoto, Japan; filter: 0.5 mm Cu and 0.5 mm Al; dose rate 0.52 Gy min^{-1}), incubated further in fresh medium, and collected at different time intervals. Proteins were then extracted using SDS buffer (50 mM Tris-HCl (pH 6.8), 2% SDS, 10% glycerol and 1% 2-mercaptoethanol). A portion of 20 μl of 2 mg ml^{-1} protein was loaded on 12% SDS-polyacrylamide gel electrophoresis, transferred to an Immobilon-P membrane (Millipore, Bedford, MA) and immunoblotted with anti-p21 mouse monoclonal antibody (BD Biosciences, Bedford, MA). Immunodetection was performed using horseradish peroxidase-conjugated secondary antibody and ECL western blotting detection reagent (GE Healthcare, Buckinghamshire, UK) on a luminescent image analyzer (LAS-1000 plus; Fuji Film, Tokyo, Japan). The densities of p21 protein bands were analyzed using Image Gauge ver.3.4 software (Fuji Film).

Tumor induction and transplantation

Male and female transgenic m*p53* mice and wild-type mice born from the same parents were used for tumor induction experiments. The MCA (Sigma-Aldrich) was dissolved in olive oil at 0.2 mg ml^{-1} and 0.1 ml of this solution was injected into the right groins of the mice at 6–8 weeks of age after individual births throughout the seasons. Tumor formation was followed by palpation for 1 year. Tumor size was measured with calipers and tumor volume was calculated by $ab^2/2$, where a and b are the lengths of the long and short axes, respectively. The day of tumor appearance was defined as the day when a tumor reached a diameter of 3 mm. When tumors were found at a larger size, this date was estimated by extrapolating tumor growth curve with a volume-doubling time of 2.5 days.[22] Tumors were sectioned, fixed with 10% formalin, stained with hematoxylin and eosin (HE) and examined histologically. Other pieces of tumors were frozen in liquid nitrogen, preserved at −80 °C and transplanted when needed. For transplantation, tumors were cut to an approximately 1 mm cube and subcutaneously transplanted in sex-matched C57BL/6J-Jcl mice using a transplantation needle with a 1.5 mm inner diameter. One of the tumors sensitive to siRNA (sequence siRNA no. 220, as described below) was transplanted serially and designated as a TT18 line.

siRNA design

The candidate nucleotide sequence for the siRNA was obtained by searching the nucleotide sequences of the chicken β-actin promoter and CMV-IE enhancer using the Qiagen program. The sequences with a high score were no. 169, CGCCAAUAGGGACUUUCCAdTdT/UGGAAAGUCCCUAUUGGCGdTdT; no. 220, CUGCCCACUUGGCAGUACAdTdT/UGUACUGCCAAGUGGGCAGdTdT; no. 290, AUGGCCCGCCUGGCAUUAUdTdT/AUAAUGCCAGGCGGGCCAUdTdT, in the CMV-IE enhancer. A high scoring sequence was not found in the chicken β-actin gene promoter.

In vitro assay of siRNA suppression activity in HEK293 cells

The pTE50 plasmids were introduced into HEK293 cells using Lipofectamine 2000 (Invitrogen), followed by selection for neo-resistant cells harboring pTE50. The cells carrying pTE50 were treated with 50 nM siRNA and 0.008% atelocollagen for 48 h at 37 °C in a humidified CO_2 incubator. Total RNA was then extracted by ISOGEN (Nippon Gene, Tokyo, Japan) and subjected to mRNA-selective PCR followed by an analysis of the products by 1% agarose gel electrophoresis. For the quantitative assay, HEK293 cells containing plasmid pCAHST-1, which carried the reporter gene human *FGF4* cDNA inserted downstream of the chicken β-actin gene promoter and CMV-IE enhancer, were treated with 50 nM siRNA and TransIT-TKO (Mirus, Madison, WI) for 48 h at 37°C ($n=3$). Total RNA was extracted using ISOGEN and treated with DNase using the TURBO-DNA free kit (Ambion, TX). RNA (2 μg) was used for the synthesis of cDNA with random primers. The cDNA was diluted 2.5-fold and 5 μl was subjected to quantitative PCR in a 50 μl reaction mixture using Platinum Quantitative PCR SuperMix-UDG (Invitrogen) and the Taq-Man Gene Expression Assay (Applied Biosystems) specific for human *FGF4* or *GAPDH*. Real-time PCR was carried out for 45 cycles of 95 °C for 15 s and 60 °C for 30 s using the ABI PRISM 7300 Sequence Detection System (Applied Biosystems). The *FGF4* expression was normalized to *GAPDH*.

Delivery of siRNA to the tumor and follow-up

Atelocollagen (Koken, Tokyo, Japan) was used to deliver siRNA to the tumors.[30] The siRNA no. 220 or nonspecific siRNA (Qiagen, cat. no. 1027281) at 0.15 mg ml^{-1} was mixed with an equal volume of 1% atelocollagen by gentle rotation for 20 min at 4°C. Autochthonous tumors were selected for treatment when they grew to a diameter of 5 mm in a spherical shape suitable for the test. Transplanted tumors usually reached this size 10 days after transplantation. Tumors were subcutaneously injected with 0.2 ml of the siRNA/atelocollagen mixture using a syringe with a 24G needle at 2–3 day intervals for a total of four injections into the tumor site. The change in the tumor size was followed by calipers measurements. The initial response was followed in both the autochthonous and transplanted tumors after the start of siRNA treatment and autochthonous tumors were followed for a cure until the death of the mice.

Apoptosis detection

Tumor tissue sections were treated by terminal deoxynucleotidyl transferase-mediated dUTP nick-end labeling (DeadEnd Fluorometric TUNEL System; Promega, Madison, WI) for 60 min at 37 °C to detect fragmented DNA, counterstained with 4′,6-diamidino-2-phenylindole

(Vector Laboratories, Burlingame, CA) and examined by microscope under UV illumination to detect apoptotic cells.

Statistical analysis of tumor incidence rate

Cumulative tumor incidence was analyzed by the Kaplan–Meier method[35] using a computer program (SSSMCTK3; Esumi, Tokyo, Japan). The difference in tumor incidence rates was evaluated by the log-rank test.

Results

Cloning of mutant p53 *cDNA and the generation of transgenic mice*

First, we cloned mutant *p53* cDNA from a mouse skin tumor produced by repeated β-irradiation.[31] This mutant *p53* contained the coding frame from exon 2 to exon 11 carrying a 9 bp deletion from codon 191 to codon 193 in exon 6,[32] which corresponds to the DNA-binding domain of the p53 protein. The 1.17 kb mutant *p53* cDNA was inserted downstream to the chicken β-actin promoter combined with the CMV-IE enhancer in the 5.8 kb expression vector pCXN2[33] to construct plasmid pTE50 (Figure 1a). When pTE50 was introduced in cultured human HEK293 cells, the mutant p53 proteins were overexpressed as revealed by abundant mutant p53 proteins by western blotting (Supplementary Figure 1). The 5.4 kb fragments of pTE50 cut with *Bam*HI/*Pvu*I were then introduced into mouse embryos at the early stage and 2 mice with the transgene were obtained out of 105 born mice, 1 of them which was male was used for breeding. The presence of the m*p53* introduced into the mouse genome was confirmed by Southern blot analysis and genomic PCR on mouse tail DNA (Figure 1b). The mRNA-selective PCR revealed that the full-length exon 2–11 m*p53* was expressed in the transgenic mice (Figure 1c). The expressions of wild-type *p53*, *p21* and chicken β-actin in the m*p53* mouse liver were also demonstrated. The presence of the 9 bp deletion from codon 191 to codon 193 in exon 6 of m*p53* mice was confirmed with the genomic DNA (data not shown) and cDNA (Figure 1d). Codon 191 was repeatedly confirmed in the wild-type mouse genomic DNA and cDNA to contain AGG (Arg) instead of CGG (Arg), which is present in the registered nucleotide sequence.

Suppressive effect of m53 *on p21 expression*

The *p53* gene activity controls the expression of the *p21* gene in the *ATM* regulating molecular network, which is involved in checkpoint arrest of the cell cycle and cellular apoptosis. The mutant *p53* could exert its activity over *p21* expression in a dominant-negative manner.[12,16,36] We examined *p21* expression in the m*p53* mouse embryonic fibroblasts after irradiation with 7 Gy. The level of p21 protein in wild-type cells increased with time, reaching a peak 6 h after irradiation, whereas the level of p21 protein in m*p53* cells increased only slightly at 3 h and then gradually decreased (Figure 2). These patterns indicate that the mutant *p53* inhibits *p21* expression in m*p53* transgenic mice in a dominant-negative manner after irradiation.

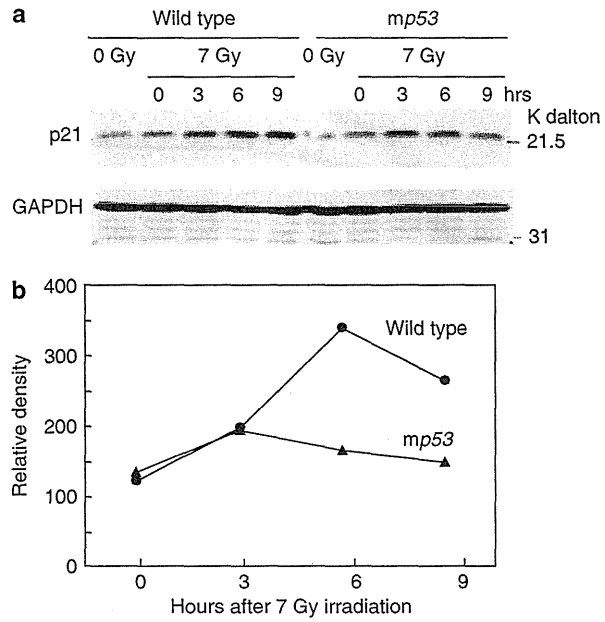

Figure 2 Effects of mutant *p53* on the expression of p21 proteins. (**a**) Cultured embryonic fibroblasts from wild-type and m*p53* transgenic mice were irradiated with 7 Gy of X-rays, and p21 protein levels were measured at different time intervals by western blotting. GAPDH was used as a loading control. (**b**) The variation in p21 protein levels shown as a function of time after irradiation. The values were normalized to GAPDH expression.

Tumor induction in m53 *transgenic mice*

The m*p53* transgenic mice and wild-type mice from the same siblings were subjected to tumor induction experiments. Mice aged 6–8 weeks were subcutaneously injected in the right groin with 20 μg MCA and followed for 1 year. The MCA dose was chosen from the dose-response data obtained with MCA-induced tumors in wild-type C3H/He mice[22] and was expected to result in a tumor incidence of 20–30%. Tumors produced with this MCA dose are monoclonal, as previously demonstrated with mosaic cell mice.[37] As shown in Figure 3, tumors started to appear in both the m*p53* and wild-type mice around day 60. The majority of tumors were fibrosarcomas of the skin, histologically. A few tumors were of other histological types, including 3 rhabdomyosarcomas and 2 squamous cell carcinomas out of the 51 tumors examined in m*p53* mice and 2 rhabdomyosarcmas out of the 52 tumors examined in wild-type mice. Spontaneous tumors never appeared on the olive oil-treated groins of the mice. The final cumulative tumor incidence for the m*p53* mice was 1.7-fold higher than that of wild-type mice (59 versus 34%; $P<0.01$). The excess tumors formed in the m*p53* mice (42% of total tumors) are, therefore, thought to be dependent on the function of mutant *p53*. Male m*p53* mice appeared to have a higher tumor

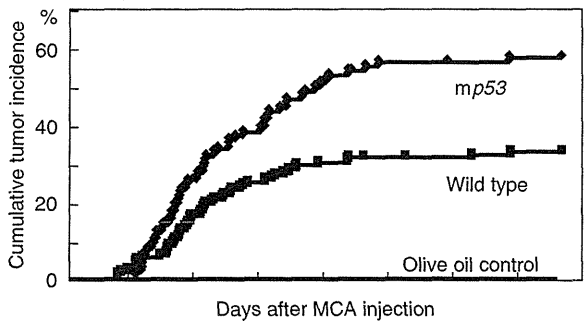

Figure 3 Cumulative tumor incidence after the subcutaneous injection of 3-methylcholanthrene (MCA). The final tumor incidence 1 year after MCA injection was 59% for transgenic m*p53* mice ($n=93$) and 34% for wild-type mice ($n=159$), a 1.7-fold difference ($P<0.01$). Control mice were injected with 0.1 ml olive oil; $n=29$ for m*p53* mice, $n=40$ for wild-type mice. Separate analyses for females and males are shown in Supplementary Figure 3.

incidence than female m*p53* mice (68 versus 48%; Supplementary Figure 3), although this difference was not statistically significant. Seasonal variation in tumor incidence was also not statistically significant (data not shown). Metastasis was absent in the lung and liver at autopsy.

As the allelic loss of wild-type *p53* tends to occur in tumors formed in *p53* heterozygous mice with a mutation on one side,[10–12] we examined the loss of wild-type *p53* alleles in tumors developed in the m*p53* mice. As determined by PCR, the wild-type *p53* gene was retained in all 20 MCA-induced tumors in the m*p53* mice (data not shown). The expression of wild-type *p53* mRNA in the representative tumor TT18 was shown for exon 4–6 (Figure 1c) or full length (data not shown).

siRNA suppression of tumor growth

The MCA-induced tumors were subjected to siRNA suppression experiments. If the m*p53*-targeting siRNA is effective in suppressing the growth of m*p53*-dependent tumors, it would be expected that the estimated 42% of tumors produced in excess in these transgenic mice will respond to the treatment and regress or at least, stop growing.

We selected siRNA no. 220 from the three candidates to suppress m*p53* expression in cultured HEK293 cells harboring pTE50 (Figure 4a) using the dose-response range (Supplementary Figure 2). The suppression activity of the siRNA was further confirmed with a reporter gene, human *FGF4*, ligated downstream of the same chicken β-actin promoter/CMV-IE enhancer as used for pTE50 in plasmid pCAHST-1. The quantitative real-time PCR analysis revealed 30% suppression ($P<0.05$), although the suppression was not complete in this system (Figure 4b).

To deliver siRNA to target molecules, an atelocollagen system, in which siRNA was complexed to atelocollagen, making it resistant to degradation *in vivo* and allowing it to be delivered stably to tumor cells, was used.[29,30] When tumors grew to a diameter of 5 mm (63 mm^3 in volume), siRNA no. 220–atelocollagen complex was injected into the site surrounding the subcutaneous solid tumor at 2–3 day intervals for a total of four injections. Control tumors were treated with negative control siRNA–atelocollagen complex. Treatments with siRNA no. 220 resulted in the suppression of the growth of 6 of 23 autochthonous tumors (26%) in the m*p53* mice, including 4 regressions and 2 growth arrests (Figure 4). Negative control siRNA had no effect on 10 tumors (Supplementary Figure 4). The regression of siRNA no. 220-sensitive tumors was rapid, and tumors became nonpalpable within 10 days of beginning of the siRNA treatment. Mice no. 1–4 survived without tumor recurrence for 110, 51, 116 and 91 days, respectively. In a strict sense, three cases, mice no. 1, 3 and 4 fit the definition of a true cure, that is, the regression of a tumor without recurrence for 60 days, a time length long enough for a single surviving tumor cell to grow to a palpable size of 3 mm in diameter with a volume-doubling time of 2.5 days.[22] Mouse no. 1 exhibited residual cell debris at the site of the tumor (Supplementary Figure 5a). The debris was stained with HE, indicating that the tumor existed there before treatment.

Another group of autochthonous tumors were individually transplanted into wild-type mice and then examined for a response to siRNA no. 220 after growing to a diameter of 5 mm. This treatment resulted in 7 responses among 21 transplants (33%). The tumor response data are summarized in Table 1. To judge the initial tumor response, the results of the transplanted tumors were combined with the results of autochthonous tumors (26%); 30% of 44 tumors in total responded to siRNA no. 220 treatment. This efficiency is approximately comparable with the population of m*p53*-dependent tumors; 42% of total tumors produced in the m*p53* mice. None of the wild-type tumors, either autochthonous or transplanted, responded to siRNA no. 220 (Table 1).

One of the tumor transplant lines, TT18, which was confirmed to be siRNA no. 220-sensitive, was observed more extensively for a response to siRNA no. 220. In TT18, the expression profiles of m*p53* and wild-type *p53* mRNAs were essentially the same as in the liver of an m*p53* mouse (Figure 1c) and genomic wild-type *p53* was preserved, as confirmed by PCR (data not shown). The TT18 tumor, after grown to a diameter of 5 mm, responded to siRNA no. 220 but not to negative control siRNA (Figure 5a). A necrotic change occurred after the treatment of TT18 with siRNA no. 220 (Supplementary Figures 5b and 5c). Concomitant with the suppression of tumor growth, the expression of m*p53* mRNA in TT18 was suppressed by treatment with siRNA no. 220 (Figure 5b). Strikingly, marked apoptosis was induced in the tumor mass during tumor regression (Figures 5c and d). Moreover, accompanied by apoptosis induction, the tissue structure of the fibrosarcoma disappeared, as demonstrated by the loss of the dense and fibrous tumor structure (Figures 5e and f).

To obtain direct evidence that siRNA no. 220 completely suppresses the growth of an m*p53*-responsive tumor without the influence of other factors, a piece of

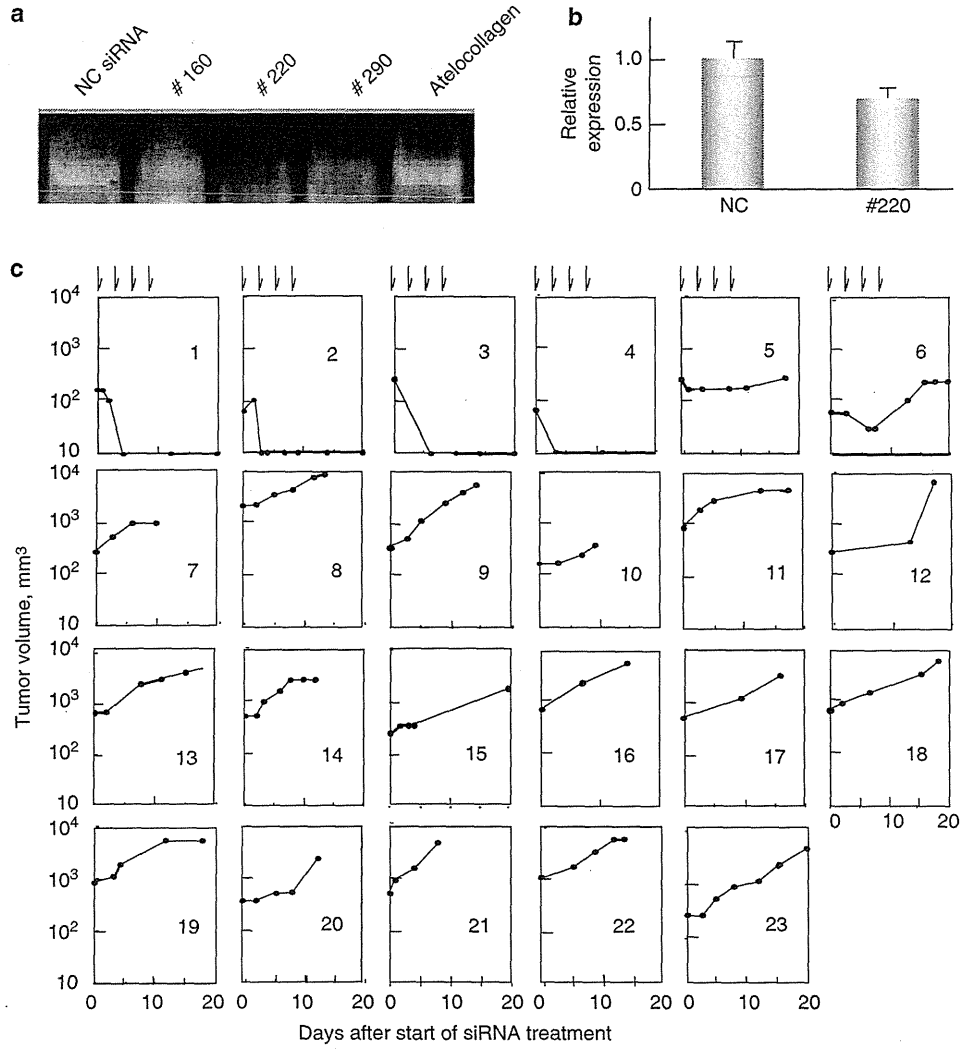

Figure 4 Selection of siRNA no. 220 and its suppressive effect on 3-methylcholanthrene (MCA)-induced autochthonous tumors in m*p53* mice. (**a**) Three candidate siRNAs and negative control (NC) siRNA, each mixed with atelocollagen, and atelocollagen alone were applied to HEK293 cells carrying pTE50. The expression of m*p53* mRNA was analyzed by mRNA-selective PCR. (**b**) siRNA no. 220 and NC siRNA were applied to HEK293 cells carrying plasmid pCAHST-1 with the reporter gene, human *FGF4*, ligated downstream of the chicken β-actin gene promoter/CMV-IE enhancer. The expression of *FGF4* mRNA was analyzed by real-time PCR and normalized to *GAPDH* expression for triplicate experiments. The mRNA expression showed a 30% suppression by siRNA no. 220 ($P<0.05$). (**c**) Tumors 5 mm or more in diameter were treated with a mixture of siRNA no. 220 and atelocollagen as indicated by arrows, and the resulting tumor growth was monitored. Mice no. 1–4 showed complete regression, mice no. 5 and 6 showed growth arrest of tumors, and mice no. 7–23 showed no suppression of tumor growth.

Table 1 Summary of the suppressive effects of siRNA no. 220 on MCA-induced tumors

Tumor	*Number of tumors examined*	*Regression*	*Growth arrest*
Induced in mp53 transgenic mice			
Autochthonous	23	4[a]	2[b]
Transplanted	21	4[c]	3[b]
Induced in wild-type mice			
Autochthonous	15	0	0
Transplanted	10	0	0

[a]Tumors regressed and did not recur for 51–116 days.
[b]Tumors stopped growing but did not regress.
[c]These tumors did not respond to nonspecific siRNA.

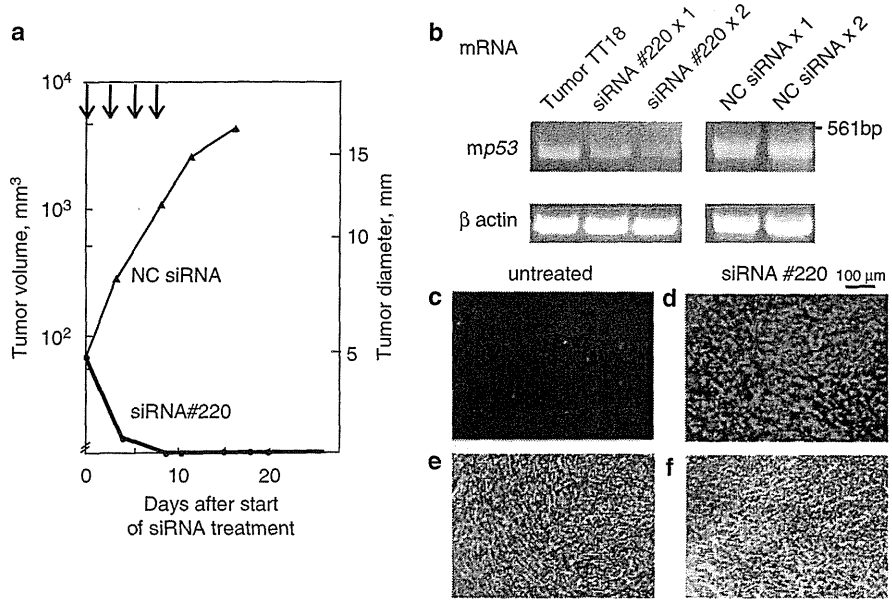

Figure 5 Effects of siRNA no. 220 on a transplanted tumor. Tumor line TT18, which was sensitive to siRNA no. 220, was used. (**a**) Change in TT18 tumor volume after treatment with siRNA no. 220 or negative control (NC) siRNA at times indicated by the arrows. The siRNA effect was confirmed in three pairs of mice; one pair is shown. (**b**) Expression profile of m*p53* mRNA from tumor TT18 after one or two treatments with siRNA no. 220 or NC siRNA, and analyzed by mRNA-selective PCR. Mouse β-actin mRNA expression was used as a control. Results were similar in duplicates; one is shown. (**c**) Terminal deoxynucleotidyl transferase-mediated dUTP nick-end labeling (TUNEL)-stained tissue section from nontreated TT18. (**d**) TUNEL-stained tissue section from TT18 after two treatments with siRNA no. 220, showing the induction of apoptosis. (**e**) Hematoxylin and eosin (HE)-stained tissue section from nontreated TT18. (**f**) HE-stained tissue section from TT18 after two treatments with siRNA no. 220, showing degradation of the fibrous structure and a loss of cell density in the fibrosarcoma.

the TT18 tumor was transplanted into the right groin of a mouse and another piece was transplanted into the left groin of the same mouse. Two days after transplantation, siRNA no. 220-atelocollagen was injected twice, at a 2-day interval, into the right transplantation site, and nonspecific siRNA-atelocollagen was simultaneously injected into the left site. Only the tumor injected with siRNA no. 220 did not grow in the right groin, whereas the tumor in the left groin injected with nonspecific siRNA grew to a diameter of 1.1 cm after 17 days, demonstrating that, in the same host, siRNA no. 220 exerts a suppressive effect at the site of injection and no effect at the site distant from the injection site in the same host. These results confirmed the effective suppression of m*p53*-dependent tumor growths by silencing the m*p53* transgene with siRNA no. 220 in the presence of wild-type *p53*.

Discussion

If mutation in the *p53* gene is a true cause of tumors, mice carrying mutant *p53* must have a high incidence of tumor development. This theme has been addressed and pursued in heterozygous mice with a *p53* mutation located in different codons corresponding to the DNA-binding domain of p53 proteins: codon 135,[7,8,11] codon 172,[11,13,14] codon 248,[12] codon 270,[10,16] codon 273[12] and codon 275.[16] These studies have shown that these *p53* mutations cause tumors.

In this study, we employed transgenic mice hemizygous for mutant *p53* carrying a deletion of codons 191–193 and retaining the wild-type *p53* alleles. The transgenic mice expressed both mutant *p53* mRNA and wild-type *p53* mRNA (Figure 1). The dominant-negative activity of mutant *p53* on p21 protein expression was confirmed in irradiated fibroblasts from the mice (Figure 2). It was expected that, during the course of tumorigenesis, the function of wild-type p53 protein would be suppressed in the transgenic mice. If the functional loss of wild-type p53 protein is responsible for tumor induction to any extent, the transgenic mice would be significantly prone to tumor induction. Consistent with this expectation, the mutant *p53* transgenic mice exhibited a significantly higher susceptibility to the chemical induction of tumors: a 1.7-fold increase in tumor incidence relative to wild-type mice when comparing the equivalent tumor induction procedure. Tumors appeared to be of two types: mutant *p53* dependent (42%) and independent. If all mutant *p53*-dependent tumors respond to the silencing of the mutant *p53*, then 42% of the total tumors produced in the transgenic mice were expected to respond and consequently regress or stop growing on siRNA treatment. The

actual gain of the response was 30% (Table 1), which seems to fit this expectation by taking into account the suppression efficiency of siRNA no. 220. The same timing for tumor appearance in m*p53* and wild-type mice (Figure 3) implies an essentially equal length of latency, indicating that the tumor increase in m*p53* mice is due to the attenuated function of wild-type *p53* in apoptosis. If the mutation affects other functions, such as cell-cycle checkpoint control or DNA repair, tumor appearance would be accelerated with a shorter latency.

In other aspects of this tumor system, MCA-induced autochthonous tumors have been a model target for experimental therapy, but curing theme is very difficult. Nakahara[21] stressed the importance of using autochthonous tumors to test agents to determine for a cure of tumors. Recently, the suppression of MCA-induced autochthonous tumors was made possible by treatment with a combination of three antibodies.[38] In this study, a further possibility was provided by gene silencing using siRNA combined with an atelocollagen delivery system. The siRNA was used to distinguish between mutant *p53* and wild-type *p53*. Atelocollagen was used to protect the siRNA from RNase attack and to efficiently deliver siRNA to the target molecules. Additionally, its cellular toxicity is weak, whereas many transfection agents are highly toxic. The tumor-specific delivery of siRNA by atelocollagen to metastatic mouse tumors *in vivo* has been demonstrated.[30] In this study, this delivery system was useful when applied to subcutaneous solid tumors. Using this method, siRNA no. 220 effectively suppressed the growth of m*p53*-dependent tumors induced with MCA, apparently overcoming the difficulty of the character of the autochthonous tumor. Although we observed only few cases of a true cure, in the strict sense, we consider these cases provide a hope for future study.

Furthermore, the transplanted tumor TT18 exhibited a drastic apoptosis induction in response to treatment with siRNA no. 220 (Figure 5c and d). This apoptosis induction is thought to be due to the restoration of wild-type *p53* activity that had been suppressed by adding mutant *p53*. In human and mouse tumors caused by *p53* mutation, the loss of wild-type *p53* often occurs during tumorigenesis, so that the restoration of apoptotic activity through the reactivation of wild-type *p53* function is impossible. In such a case, it will be necessary to further develop a molecular devise to compensate for wild-type *p53* function or to activate apoptosis by other means.

In conclusion, we demonstrated that the mutant *p53* with a 9 bp deletion in exon 6 elevates tumor incidence in the presence of wild-type p53 alleles, and that these tumors can be suppressed by silencing the mutant *p53* transgene and, thereby, reactivating the apoptotic capacity. The results point out a new and promising modality toward the cure of human cancers, especially when the causative overexpressing gene can be identified.

Conflict of interest

The authors declare no conflict of interest.

Acknowledgements

We thank Dr S Kondo for his continuous encouragement and critical comments, Dr S Takahashi for his support of this study, Dr M Katsuki for useful suggestions, Dr K Hirai and Dr K Maruyama for technical advice and support, and Dr S Kito and Ms Y Oota for preparing frozen transgenic mouse embryos. This work was supported by a Grant-in-Aid for Cancer Research from the Ministry of Health and Welfare, Japan, a Special Grant for the Project Research 'Genetic Control of Biodefense Mechanisms against Radiation' (KT), a Grant-in-Aid for Scientific Research from the Ministry of Education, Culture, Sports, Science and Technology, Japan (KT), a Grant-in-Aid for the Third-Term Comprehensive 10-Year Strategy for Cancer Control (TO) and the Program for the Promotion of Fundamental Studies in Health Sciences of the National Institute of Biomedical Innovation (TO).

References

1 Levine AJ. *p53*, the cellular gatekeeper for growth and division. *Cell* 1997; **88**: 323–331.
2 Pietsch EC, Sykes SM, McMahon SB, Murphy ME. The *p53* family and programmed cell death. *Oncogene* 2008; **27**: 6507–6521.
3 Norimura T, Nomoto S, Kikuchi M, Gondo Y, Kono S. *p53*-dependent apoptosis suppresses radiation-induced teratogenesis. *Nat Med* 1996; **2**: 577–580.
4 Hu W, Feng Z, Teresky AK, Levine AJ. *p53* regulates maternal reproduction through LIF. *Nature* 2007; **450**: 721–724.
5 Holstein M, Sidransky D, Vogelstein B, Harris CC. *p53*: mutations in human cancers. *Science* 1991; **253**: 49–53.
6 Malkin D. Germ line p53 mutations and heritable cancers. *Annu Rev Genet* 1994; **28**: 443–465.
7 Lavigueur A, Maltby V, Mock D, Rossant J, Pawson T, Bernstein A. High incidence of lung, bone, and lymphoid tumors in transgenic mice overexpressing mutant alleles of the *p53* oncogene. *Mol Cell Biol* 1989; **9**: 3982–3991.
8 Harvey M, Vogel H, Morris D, Bradley A, Bernstein A, Donehower LA. A mutant *p53* transgene accelerates tumour development in heterozygous but not nullizygous *p53*-deficient mice. *Nat Gen* 1995; **9**: 305–311.
9 Zhang Z, Li J, Lantry LE, Wang Y, Wiseman RW, Lubet RA *et al. p53* transgenic mice are highly susceptible to 1,2-dimethylhydrazine-induced uterine sarcomas. *Cancer Res* 2002; **62**: 3024–3029.
10 Olive KP, Tuveson DA, Ruhe ZC, Yin B, Willis NA, Bronson RT *et al.* Mutant *p53* gain of function in two mouse models of Li-Fraumeni syndrome. *Cell* 2004; **119**: 847–860.
11 Lang GA, Iwakura T, Suh YA, Liu G, Rao A, Parant JM *et al.* Gain of functon of a *p53* hot spot mutation in a mouse model of Li-Fraumeni syndrome. *Cell* 2004; **119**: 861–872.
12 Song H, Hollstein M, Xu Y. *p53* gain-of-function cancer mutants induce genetic instability by inactivating ATM. *Nat Cell Biol* 2007; **9**: 573–580.
13 Liu G, McDonnel TJ, Montes de Oca Luna R, Kapoor M, Mims B, El-Naggar B *et al.* High metatstatic potential in mice inheriting a targeted *p53* missense mutation. *Proc Natl Acad Sci USA* 2000; **97**: 4174–4179.

14 Wang XJ, Greenhalgh DA, Jiang A, He D, Zhong L, Medina D *et al.* Expression of a *p53* mutant in the epidermis of transgenic mice accelerates chemical carcinogenesis. *Oncogene* 1998; **17**: 35–45.
15 Kern SE, Pietenpol JA, Thiagalingam S, Seymour A, Kinzler KW, Vogelstein B. Oncogenic forms of *p53* inhibit *p53*-regulated gene expression. *Science* 1991; **256**: 827–830.
16 de Vries A, Flores E, Miranda B, Hsieh HM, van Oostrom CTM, Sage J *et al.* Targeted point mutations of *p53* lead to dominant-negative inhibition of wild-type *p53* function. *Proc Natl Acad Sci USA* 2002; **99**: 2948–2953.
17 Donehower LA, Harvey M, Slagel BL, McArthur MJ, Montgomery Jr CA, Buttel JS *et al.* Mice deficient for *p53* are developmentally normal but susceptible to spontaneous tumors. *Nature* 1992; **356**: 215–221.
18 Kemp CJ, Donehower LA, Bradley A, Balmain A. Reduction of *p53* gene dosage does not increase initiation or promotion but enhances malignant progression of chemically induced skin tumorigenesis. *Cell* 1993; **74**: 813–822.
19 Ventura A, Kirsch DG, McLaughin ME, Trveson DA, Grim J, Lintault L *et al.* Restoration of *p53* function leads to tumour regression *in vivo*. *Nature* 2007; **445**: 661–665.
20 Xue W, Zender L, Miething C, Dickins RA, Herando E, Krizhanovsky V *et al.* Senescence and tumour clearance is triggered by *p53* restoration in murine liver carcinomas. *Nature* 2007; **445**: 656–660.
21 Nakahara W. A pilgrim's progress in cancer research, 1918 to 1974: autobiographical essay. *Cancer Res* 1974; **34**: 1767–1774.
22 Tanooka H, Tanaka K, Arimoto H. Dose response and growth rates of subcutaneous tumors induced with 3-methylcholanthrene in mice and timing of tumor origin. *Cancer Res* 1982; **42**: 4740–4743.
23 Tanooka H, Hoshino H, Tanaka K, Nagase M. Experimental radiation therapy and apparent radioresistance of autochthonous tumors subcutaneously induced with 3-methylcholanthrene in mice. *Cancer Res* 1980; **40**: 2547–2551.
24 Tanooka H, Tanaka K. Test of recurrence after experimental radiation therapy of chemically induced autochthonous tumors in mosaic mice. *Int J Radiat Oncol Biol Phys* 1985; **11**: 1551–1555.
25 Koebel CM, Vermi W, Swann JB, Zerafa N, Rodig SJ, Old LJ *et al.* Adaptive immunity maintains occult cancer in an equilibrium state. *Nature* 2007; **450**: 903–908.
26 Meister G, Tuschl T. Mechanisms of gene silencing by double-stranded RNA. *Nature* 2004; **431**: 343–349.
27 Morris KV, Simon W-L, Jacobson SE, Looney DJ. Small interfering RNA-induced transcriptional gene silencing in human cells. *Science* 2004; **305**: 1289–1292.
28 Kim DH, Villeneuve LM, Morris KV, Rossi JJ. Argonaute-1 directs siRNA-mediated transcriptional gene silencing in human cells. *Nat Struct Biol* 2006; **13**: 793–797.
29 Minakuchi Y, Takeshita F, Kosaka N, Sasaki H, Yamamoto Y, Kouno M *et al.* Atelocollagen-mediated synthetic small interfering RNA delivery for effective gene silencing *in vitro* and *in vivo*. *Nucleic Acids Res* 2004; **32**: e109.
30 Takeshita F, Minakuchi Y, Nagahara S, Honma K, Sasaki, Hirai K *et al.* Efficient delivery of small interfering RNA to bone-metastatic tumors by using atelocollagen *in vivo*. *Proc Natl Acad Sci USA* 2005; **102**: 12177–12182.
31 Ootsuyama A, Tanooka H. One hundred percent tumor induction in mouse skin after repeated β irradiation in a limited dose range. *Radiat Res* 1988; **115**: 488–494.
32 Ootsuyama A, Makino H, Nagao M, Ochiai A, Yamauchi, Tanooka H. Frequent *p53* mutation in mouse tumors induced by repeated β-irradiation. *Mol Carcinog* 1994; **11**: 236–242.
33 Niwa H, Yamamura K, Miyazaki J. Efficient selection for high-expression transfectants with a novel eukaryotic vector. *Gene* 1991; **108**: 193–200.
34 Auer T, Sninsky JJ, Gelfand DH, Myers TW. Selective amplification of RNA utilizing the nucleotide analog dITP and *Thermus thermophilus* DNA polymerase. *Nucleic Acids Res* 1996; **24**: 5021–5025.
35 Hoel DG, Walburg HE. Statistical analysis of survival experiments. *J Natl Cancer Inst* 1972; **49**: 361–372.
36 El-Deiry WS, Tokino T, Velculescu VE, Levy DB, Parsons R, Trent JM *et al.* WAF1, a potential mediator of *p53* tumor suppression. *Cell* 1993; **75**: 817–825.
37 Tanooka H, Tanaka K. Dose response of monoclonal tumor induction with 3- methylcholanthrene in mosaic mice. *Cancer Res* 1984; **44**: 4630–4632.
38 Uno T, Takeda K, Kojima Y, Yoshizawa H, Akiba H, Mittler RS *et al.* Eradication of established tumors in mice by a combination antibody-based therapy. *Nat Med* 2006; **12**: 693–698.

Supplementary Information accompanies the paper on Cancer Gene Therapy website (http://www.nature.com/cgt)

Strong interaction between the effects of alcohol consumption and smoking on oesophageal squamous cell carcinoma among individuals with *ADH1B* and/or *ALDH2* risk alleles

Fumiaki Tanaka,[1] Ken Yamamoto,[2] Sadao Suzuki,[3] Hiroshi Inoue,[1] Masahiko Tsurumaru,[4] Yoshiaki Kajiyama,[4] Hoichi Kato,[5] Hiroyasu Igaki,[5] Koh Furuta,[6] Hiromasa Fujita,[7] Toshiaki Tanaka,[7] Yoichi Tanaka,[8] Yoshiyuki Kawashima,[8] Shoji Natsugoe,[9] Tetsuro Setoyama,[9] Shinkan Tokudome,[3] Koshi Mimori,[1] Naotsugu Haraguchi,[1,10] Hideshi Ishii,[1,10] Masaki Mori[1,10]

► Additional figures and tables are published online only. To view these files please visit the journal online (http://gut.bmj.com).

[1]Department of Surgery, Medical Institute of Bioregulation, Kyushu University, Beppu, Japan
[2]Department of Molecular Genetics, Medical Institute of Bioregulation, Kyushu University, Fukuoka, Japan
[3]Department of Public Health, Nagoya City University Graduate School of Medical Sciences, Nagoya, Japan
[4]Department of Esophageal and Gastroenterological Surgery, Juntendo University School of Medicine, Tokyo, Japan
[5]Department of Surgery, National Cancer Center Hospital, Tokyo, Japan
[6]Division of Clinical Laboratories, National Cancer Center Hospital, Tokyo, Japan
[7]Department of Surgery, Kurume University School of Medicine, Kurume, Japan
[8]Division of Gastroenterological Surgery, Saitama Cancer Center, Saitama, Japan
[9]Department of Surgical Oncology and Digestive Surgery, Kagoshima University School of Medicine, Kagoshima, Japan
[10]Department of Gastroenterological Surgery, Osaka University Graduate School of Medicine, Osaka, Japan

Correspondence to
Dr Masaki Mori, Department of Gastroenterological Surgery, Osaka University Graduate School of Medicine, 2-2 Yamadaoka, Suita, Osaka, Japan 565-0871; *mmori@gesurg.med.osaka-u.ac.jp*

Revised 5 July 2010
Accepted 8 July 2010
Published Online First 9 September 2010

ABSTRACT

Background Oesophageal squamous cell carcinoma (OSCC) is considered a difficult cancer to cure. The detection of environmental and genetic factors is important for prevention on an individual basis.

Objective To identify groups at high risk for OSCC by simultaneously analysing both genetic and environmental risk factors.

Methods A multistage genome-wide association study of OSCC in Japanese individuals with a total of 1071 cases and 2762 controls was performed.

Results Two associated single-nucleotide polymorphisms (SNPs), as well as smoking and alcohol consumption, were evaluated as genetic and environmental risk factors, respectively, and their interactions were also evaluated. Risk alleles of rs1229984 (*ADH1B*) and rs671 (*ALDH2*) were highly associated with OSCC (odds ratio (OR)=4.08, $p=4.4\times10^{-40}$ and OR=4.13, $p=8.4\times10^{-76}$, respectively). Also, smoking and alcohol consumption were identified as risk factors for OSCC development. By integrating both genetic and environmental risk factors, it was shown that the combination of rs1229984 and rs671 risk alleles with smoking and alcohol consumption was associated with OSCC. Compared with subjects with no more than one environmental or genetic risk factor, the OR reached 146.4 (95% CI 50.5 to 424.5) when both environmental and genetic risk factors were present. Without the genetic risks, alcohol consumption did not correlate with OSCC. In people with one or two genetic risk factors, the combination of alcohol consumption and smoking increased OSCC risk.

Conclusions Analysis of *ADH1B* and *ALDH2* variants is valuable for secondary prevention of OSCC in high-risk patients who smoke and drink alcohol. In this study, SNP genotyping demonstrated that the *ADH1B* and/or *ALDH2* risk alleles had an interaction with smoking and, especially, alcohol consumption. These findings, if replicated in other groups, could demonstrate new pathophysiological pathways for the development of OSCC.

Significance of this study

What is already known about this subject?

► Oesophageal squamous cell carcinoma (OSCC) is associated with drinking and smoking alcohol, but the genetic risk is unknown.

What are the new findings?

► This study demonstrates that single nucleotide polymorphisms of *ADH1B* and *ALDH2* interact with alcohol consumption, especially when combined with smoking, to increase OSCC risk.

How might they impact on clinical practice in the foreseeable future?

► The analysis of *ADH1B* and *ALDH2* variants would be valuable for individualised prevention of OSCC.

INTRODUCTION

Oesophageal squamous cell carcinoma (OSCC), but not adenocarcinoma, is relatively common in East Asia, including Japan.[1] Oesophageal cancer is the eighth most common cancer world wide, accounting for 462 000 new cases in 2002, and the sixth most common cause of cancer-related death (386 000 deaths). OSCC is the most common histological type world wide,[2] and is a treatment-resistant cancer that can withstand a combination of surgery, chemotherapy and radiotherapy.[1] It is difficult to diagnose OSCC early because it shows few symptoms in its early stages. Furthermore, there is no effective marker for predicting the development of OSCC. Therefore, it is important to detect risk factors for primary prevention and also to identify high-risk groups for secondary prevention.

Both genetic and environmental factors are involved in the pathogenesis of OSCC. Although smoking and alcohol consumption have been demonstrated as lifestyle factors that contribute to the development of the disease,[3] the DNA sequence variations that confer an additional risk of developing the disease remain largely unknown. The availability of high-resolution linkage disequilibrium (LD) maps and comprehensive sets of common single nucleotide polymorphisms (SNPs) that capture most of the common sequence

variations facilitate the identification of disease-related genes with genome-wide association studies, an approach without an a priori hypothesis based on a gene function or disease pathway.

To identify OSCC-related genes, we conducted a multistage genome-wide association study in Japanese individuals, with a total of 1071 cases and 2762 controls, and identified a significant genome-wide level of association for two and six SNPs on chromosomes 4q23 and 12q24.11-13, respectively. The most functional variants in the two regions, rs1229984 (*ADH1B*) and rs671 (*ALDH2*),[4] were strongly associated with OSCC. Furthermore, we analysed the association with OSCC of smoking and drinking alcohol, two of the principal environmental determinants of OSCC, both individually and jointly.[5] Finally, we evaluated the combined effects of environmental and genetic risk factors.

METHODS

Study sample

This case–control study was designed to investigate the environmental and genetic risk factors for OSCC. The eligibility criterion was that the oesophageal disease was pathologically diagnosed as OSCC. Patients with newly diagnosed oesophageal cancer, 35–85 years of age, were identified from six hospitals (Juntendo University Hospital, National Cancer Center Hospital, Kurume University Hospital, Saitama Cancer Center, Kagoshima University Hospital and Kyushu University Hospital) from 2000 to 2008. Healthy controls without a previous cancer history were recruited from Kyushu University Hospital (and related hospitals) during the same time period. All controls were enrolled after receiving an upper gastrointestinal endoscopy test to ensure that they had no disease. All participants provided written informed content. The study protocol was reviewed and approved by Kyushu University (Fukuoka, Japan), Juntendo University (Tokyo, Japan), National Cancer Center Hospital (Tokyo, Japan), Kurume University (Kurume, Japan), Saitama Cancer Center (Saitama, Japan) and Kagoshima University (Kagoshima, Japan). In total, 1071 patients with OSCC and 2762 controls were enrolled.

Environmental risk factors

Detailed information about demographic characteristics, lifestyle and daily diet was collected using a standardised questionnaire. Of all the known determinants of OSCC, we chose the two major ones—smoking and alcohol consumption—as environmental risk factors to investigate in detail. Information on smoking and alcohol consumption habits (eg, current smoker, ex-smoker, or non-smoker for smoking status) was collected at the time of enrolment. In addition, the Brinkman index (product of the number of cigarettes per day and years of smoking) for current smokers and years after quitting smoking or drinking (<1 year, 1–2 years, 3–9 years, or 10 years or longer) were calculated. Of the data collected from 1071 patients with OSCC and 2762 controls, the data from 742 patients with OSCC and 820 controls were analysed.

Genotyping, quality control and genetic association analysis

The genome-wide association study was carried out using the Affymetrix GeneChip Human Mapping 500K array (online supplementary figure 1). We genotyped 226 OSCC cases and 1118 controls using the Bayesian Robust Linear Model with Mahalanobis (BRLMM) algorithm. Samples with a genotype call rate <0.94 for either *Nsp*I or *Sty*I GeneChip SNPs were removed from analysis (N=12). To detect duplicated samples, relatives, and DNA-contaminated samples, pairwise identity-by-descent (IBD) estimation was carried out. We detected 1, 28 and 2 pairs showing IBD (PI_HAT) proportions of 1.0, approximately 0.5 and 0.25, respectively. Based on the results, 31 samples that had lower genotype call rates in each pair were excluded from the association analysis. In addition, we removed samples that had deviated averages of PI_HAT (approximately more than 3 standard deviations (PI_HAT > 0.020, N=13, see supplementary figure 2)) because such high mean PI_HAT values might be caused by DNA contamination or low-quality genotyping. These 13 samples also had higher rates of heterozygous genotypes than the other study samples (supplementary figure 3). After the sample quality check, 1288 samples (209 OSCC and 1079 controls) were subjected to further analysis.

SNPs were removed from analysis if they had a call rate of less than 0.95, showed a difference in call rate of more than 0.03 between OSCC and controls, displayed Hardy–Weinberg disequilibrium ($p<1.0\times10^{-4}$) in the control group, or had a minor allele frequency (MAF) <0.10. SNPs that were not selected in the updated GeneChip SNP5.0 (Affymetrix) were also excluded. After these exclusions, 234 830 SNPs remained in the first stage. The genomic inflation factor based on the median χ^2 value was 1.024 in this genome-wide association analysis (supplementary figure 4), implying that there was no systematic increase of false positives owing to population stratification or to any other form of bias. Six SNPs on chromosome 12q24 were strongly associated with the disease, exceeding the genome-wide significance level of $p=1.0\times10^{-7}$ (supplementary figure 5).

In the second stage, 480 OSCC and 864 control samples were genotyped using the Illumina Golden Gate Assay for the best 1536 SNPs (allelic p<0.013). When multiple SNPs displayed strong LD with each other ($r^2>0.8$), the most closely associated SNP was chosen to avoid redundancy during the selection of the 1536 SNPs. The samples with a genotype call rate <0.98 and SNPs with a call rate <0.98, Hardy-Weinberg disequilibrium ($p<1.0\times10^{-4}$) in the controls, or an MAF <0.05 were excluded from the association analysis. After quality control, 479 OSCC, 863 control and 1419 SNP samples remained, and 66 SNPs had an allele test p<0.05 at this stage.

Among the 26 SNPs that showed an allelic p<0.01 in the second stage, 25 could be genotyped with the TaqMan method in 365 OSCC cases and 780 controls in the third stage. The average SNP call rate of these 25 SNPs was 0.998. We identified 10 SNPs with an allelic p<0.05, and eight SNPs reached a significant genome-wide association level ($p<1\times10^{-7}$) in combined samples. The non-synonymous SNPs rs1229984 (*ADH1B*), rs671 (*ALDH2*) and rs16969968 (*CHRNA5*), as well as the synonymous SNP rs1051730 (*CHRNA3*), were also genotyped in all samples in the first through third stages by the TaqMan method.

Statistical analysis

To evaluate genetic and environmental factors, genotype data for the two SNPs (rs1229984 and rs671) and lifestyle data (smoking and alcohol consumption) were available for 742 OSCC cases and 820 controls. Odds ratios (OR) and 95% CIs (95% CIs) were calculated using unconditional logistic regression models, adjusted for sex, age (5-year categories) and study area (Honshu and Kyushu islands).

The environmental factors—that is, history of smoking and alcohol consumption, were re-categorised into two subclasses according to whether subjects had a previous habit of smoking or drinking; this was done to minimise the effect of disease. To evaluate the interaction effect more simply, we chose the

dominant or recessive model for both SNPs, combining the heterozygous group into either a wild homozygous or mutant homozygous group. The model was selected based on the fitness of the logistic regression. For the results, subjects with GA at rs1229984 were included in the group of AA homozygotes because the recessive model was a better fit than the dominant model. In contrast, the AG and AA genotypes of rs671 were combined because the dominant model was a better fit.

First, we estimated the environmental risk arising from smoking and alcohol consumption both individually and in combination (risk=0, 1 or 2). Similarly, for genetic risk, we estimated the OR of each factor of rs671 (AG/AA) and rs1229984 (GG) and their combined effect (risk=0, 1 or 2). Next, we repeated the same analysis for environmental risk according to the stratum of genetic risk. In the stratified analysis, we evaluated how the environmental effect was modified in the different genetic strata—that is, the existence of a gene–environment interaction. Here we used subjects with the AG/AA genotype of rs671 and/or GG genotype of rs1229984 as a genetic risk group. Finally, we calculated the risk number for the four risk factors in comparison with subjects who had no risk factors to evaluate the accumulation of risk (risk=0, 1, 2, 3 or 4) (tables 1, 2, and 3 and Figure 1).

p Values for the interaction are based on likelihood ratio tests that compared models with and without interaction terms.

Table 1 Characteristics of the cases and controls

Characteristics	Cases (N=742)		Controls (N=820)	
Sex				
Male	641	(86.4)	506	(61.7)
Female	101	(13.6)	314	(38.3)
Age (years)				
40–49	24	(3.2)	127	(15.5)
50–59	149	(20.1)	247	(30.1)
60–69	330	(44.5)	256	(31.2)
70–79	239	(32.2)	190	(23.2)
Environmental risk factor				
Non-drinker	63	(8.5)	341	(41.6)
Ever-drinker (environmental risk)	679	(91.5)	479	(58.4)
Non-smoker	103	(13.9)	422	(51.5)
Ever-smoker (environmental risk)	639	(86.1)	398	(48.5)
Environmental risk No=0	36	(4.9)	252	(30.7)
Environmental risk No=1	94	(12.7)	259	(31.6)
Environmental risk No=2	612	(82.5)	309	(37.7)
Genetic risk factor				
rs671 GG	194	(26.1)	502	(61.2)
rs671 AG/AA (genetic risk)	548	(73.9)	318	(38.8)
rs1229984 AA/AG	591	(79.6)	776	(94.6)
rs1229984 GG (genetic risk)	151	(20.4)	44	(5.4)
Genetic risk No=0	169	(22.8)	479	(58.4)
Genetic risk No=1	447	(60.2)	320	(39.0)
Genetic risk No=2	126	(17.0)	21	(2.6)
Total risk				
Total risk No=0	15	(2.0)	115	(14.0)
Total risk No=1	44	(5.9)	266	(32.4)
Total risk No=2	187	(25.2)	348	(42.4)
Total risk No=3	385	(51.9)	87	(10.6)
Total risk No=4	111	(15.0)	4	(0.5)

Results are shown as number (%).
No: The environmental risk arising from smoking and alcohol consumption, both individually and in combination (risk=0, 1 or 2). Similarly, for the genetic risk of each factor of rs671 (AG/AA) and rs1229984 (GG) and their combined effect (risk=0, 1 or 2). Finally, we calculated the risk number for the four risk factors in comparison with subjects who had no risk factors to evaluate the accumulation of risk (risk=0, 1, 2, 3 or 4).

Table 2 Risk of oesophageal squamous cell carcinoma associated with environmental and genetic risk factors and their internal interaction

Risk factors	Cases	Controls	OR	95% CI
Environmental risk factor				
Non-drinker and non-smoker (environmental risk No=0)	36	252	1.0	Reference
Ever-drinker and non-smoker (environmental risk No=1)	67	170	3.5	(2.1 to 5.8)
Non-drinker and ever-smoker (environmental risk No=1)	27	89	2.3	(1.2 to 4.3)
Ever-drinker and ever-smoker (environmental risk No=2)	612	309	16.0	(9.7 to 26.3)
p Value for interaction of drinking and smoking			0.048	
Genetic risk factor				
rs671 GG and rs1229984 AA/AG (genetic risk No=0)	169	479	1.0	Reference
rs671 AG/AA and rs1229984 AA/AG (genetic risk No=1)	422	297	4.8	(3.7 to 6.3)
rs671 GG and rs1229984 GG (genetic risk No=1)	25	23	3.1	(1.6 to 6.1)
rs671 AG/AA and rs1229984 GG (genetic risk No=2)	126	21	34.0	(18.1 to 63.8)
p Value for interaction of two genetic factors			0.079	

The odds ratios and the 95% CIs for oesophageal squamous cell carcinoma associated with alcohol consumption, smoking, and single nucleotide polymorphisms were estimated from logistic regression models adjusted for sex, age and study area. No: The environmental risk arising from smoking and alcohol consumption, both individually and in combination (risk=0, 1 or 2). Similarly, for the genetic risk of each factor—rs671 (AG/AA) and rs1229984 (GG)—and their combined effect (risk=0, 1 or 2). Finally, we calculated the risk number for the four risk factors in comparison with subjects who had no risk factors to evaluate the accumulation of risk (risk=0, 1, 2, 3 or 4).

Statistical analyses were performed with SAS software version 9.1 (SAS Institute). A two-tailed p value of <0.05 was considered statistically significant.

Genotype data cleaning and IBD analysis were carried out using PLINK version 1.06 software.[6] LD was assessed with HaploView version 4.0.[7] The statistical power for the allelic association analysis in the first and second stages of this study was calculated using the PS program[8] (supplementary table 1). Statistical analyses for the gene–environment interaction were performed with SAS. A two-tailed p value of <0.05 was considered statistically significant.

RESULTS

Figure 2 shows the study design. Table 1 shows several characteristics of the cases and controls. Cases included more men, older individuals, ever-drinkers, ever-smokers and subjects with the AG/AA genotype of rs671 and GG genotype of rs1229984 than controls. The average risk was significantly higher among cases (2.7) than among controls (1.5).

Our multistage association study identified two and six SNPs on chromosomes 4q23 and 12q24.11-13, respectively, which showed genome-wide evidence for association with OSCC ($p<1.0\times10^{-7}$) (table 4). The disease-associated markers of 4q23 spanned the *ADH* gene cluster region, including seven *ADH* family genes: *ADH1A, ADH1B, ADH1C, ADH4, ADH5, ADH6* and *ADH7* (Figure 3). We searched for functional SNPs in these genes in the SNP database and found one validated non-synonymous SNP in exon 3 of *ADH1B*, rs1229984, with an MAF >0.1 in the East Asian population. In addition, 12q24.12 contains the *ALDH2* gene, which is a well-known key enzyme in alcohol metabolism (Figure 4). This gene also possesses a non-synonymous SNP in exon 12, rs671, that affects its enzymatic activity. We assessed the LD between these functional SNPs and

Table 3 The risk of oesophageal squamous cell carcinoma associated with alcohol consumption and smoking status

Risk factors	rs671 GG and rs1229984 AA/AG (genetic risk No =0)		rs671 AG/AA or rs1229984 GG (genetic risk No=1 or 2)		p Value for interaction*
	OR	95% CI	OR	95% CI	
Environmental risk factor					
Non-drinker and non-smoker (environmental risk No=0)	1.0	Reference	1.1	(0.5 to 2.4)	
Ever-drinker and non-smoker (environmental risk No=1)	1.5	(0.7 to 3.3)	12.1	(5.5 to 26.6)	<0.001
Non-drinker and ever-smoker (environmental risk No=1)	4.5	(1.3 to 15.9)	2.4	(1.1 to 5.3)	0.44
Ever-drinker and ever-smoker (environmental risk No=2)	5.0	(2.5 to 10.1)	62.1	(30.3 to 127.4)	<0.001
p Value for interaction of drinking and smoking	0.55		0.048		

The odds ratios and 95% confidence intervals for oesophageal squamous call carcinoma associated with alcohol consumption and smoking were estimated from logistic regression models adjusted for sex, age, mutual habit and study area.
*p Value for interaction between genetic risk and drinking and/or smoking status.

associated SNP markers. We detected moderate LD between rs1229984 and rs1042026 as well as between rs671 and rs11066280 (r^2=0.66 and 0.87, respectively) in control samples (supplementary figure 5). These observations led us to examine the association of rs1229984 and rs671 with OSCC. We found a stronger association between these SNPs and OSCC (allele test OR=1.82, p $=6.2\times10^{-28}$ and OR =1.78, p $=1.0\times10^{-26}$ for rs1229984 and rs671, respectively) than between marker SNPs and OSCC (allele test OR=1.66, p$=1.8\times10^{-16}$ and OR=1.68, p$=2.5\times10^{-21}$ for rs1042026 on 4q23 and rs11066280 on 12q24, respectively), suggesting that rs1229984 and rs671 might be susceptibility variants for OSCC (table 4). Because the other SNP markers with disease associations reside in introns (eg, rs3805322 and rs2074356 reside in the introns of *ADH4* and *C12orf51*, respectively), we cannot exclude the possibility that they have a biological effect on genes from this region. However, other lines of evidence support a possible role for *ADH1B* and *ALDH2* in the pathogenesis of OSCC.

The risk alleles of rs1229984 in *ADH1B* (G) and rs671 in *ALDH2* (A) encode arginine-48 and lysine-504, respectively,

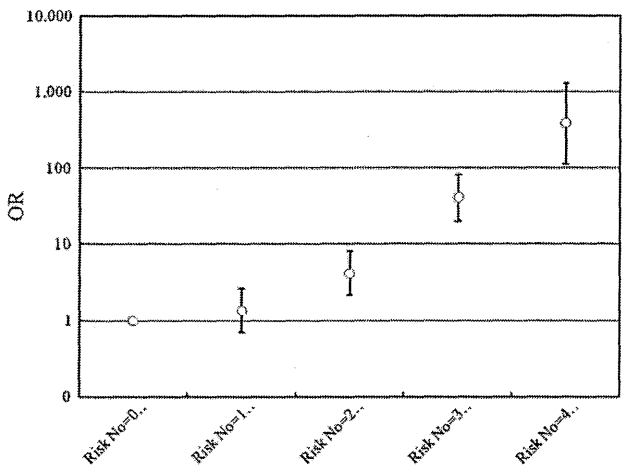

Figure 1 Magnitude of the risk of oesophageal squamous cell carcinoma (OSCC) associated with the number of environmental and genetic risk factors. The odds ratios (ORs) and the 95% CIs for OSCC associated with alcohol consumption, smoking and single nucleotide polymorphisms (rs671 GG and rs1229984) are estimated from logistic regression models adjusted for sex, age and study area. The data are shown as OR+95% CI. No: The environmental risk arising from smoking and alcohol consumption, both individually and in combination (risk=0, 1 or 2). Similarly, for the genetic risk of each factor—rs671 (AG/AA) and rs1229984 (GG)—and their combined effect (risk=0, 1 or 2). Finally, we calculated the risk number for the four risk factors in comparison with subjects who had no risk factors to evaluate the accumulation of risk (risk=0, 1, 2, 3 or 4).

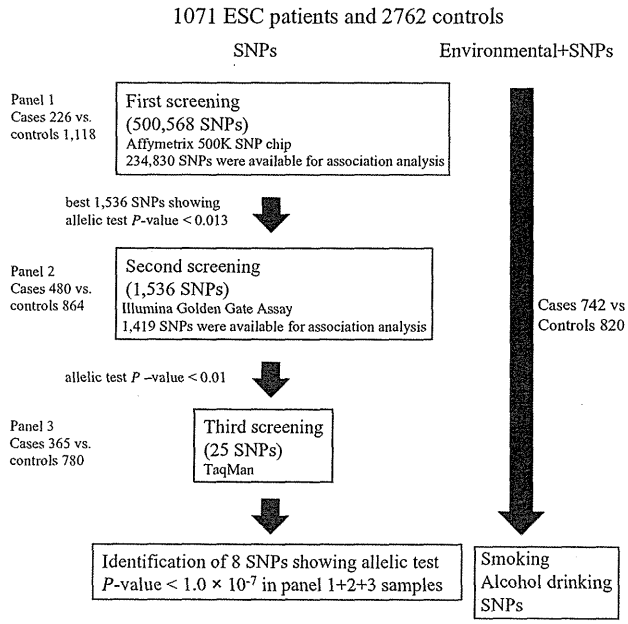

Figure 2 Design of the genome-wide association study and gene-environmental interaction study. In the first stage, 226 patients with oesophageal squamous cell carcinoma (ESC) and 1118 controls were genotyped for 500 568 single nucleotide polymorphisms (SNPs) by Affymetrix 500 K chip sets. Two additional rounds of screening by the Illumina Golden Gate Assay (1536 SNPs for the second screening) and TaqMan Assay (25 SNPs for the third screening) were performed as indicated. To evaluate genetic and environmental factors, genotype data for the two SNPs (rs1229984 and rs671) and lifestyle data (smoking and alcohol consumption) were available for 742 patients with ESC and 820 controls.

Table 4 Association of single nucleotide polymorphisms (SNPs) at 4q23 and 12q24 with oesophageal squamous cell carcinoma (OSCC) in the Japanese samples

SNP (Chromosome; position*)	Screening stage†	Risk allele frequency		OR (95% CI)‡	p Value‡	Genotyping success rate (%)	
		OSCC	Control			OSCC	Control
rs3805322	First	0.45	0.38	1.35 (1.09 to 1.66)	0.0056	100	100
(Chr.4; 100276021)	Second	0.47	0.39	1.42 (1.21 to 1.67)	1.5×10^{-5}	100	100
	Third	0.47	0.35	1.65 (1.38 to 1.97)	4.1×10^{-8}	100	100
	Combined	0.47	0.37	1.48 (1.34 to 1.64)	4.5×10^{-14}	100	100
rs1042026	First	0.22	0.16	1.47 (1.13 to 1.90)	0.0038	100	99.6
(Chr.4; 100447489)	Second	0.26	0.18	1.53 (1.26 to 1.85)	1.0×10^{-5}	99.8	100
	Third	0.26	0.16	1.83 (1.48 to 2.26)	1.9×10^{-8}	99.7	99.9
	Combined	0.25	0.17	1.66 (1.47 to 1.88)	1.8×10^{-16}	99.8	99.8
rs2238149	First	0.30	0.19	1.79 (1.41-2.27)	1.1×10^{-6}	99.0	98.2
(Chr.12; 109796312)	Second	0.26	0.21	1.32 (1.10 to 1.59)	0.0031	100	100
	Third	0.24	0.20	1.26 (1.02 to 1.56)	0.032	100	99.9
	Combined	0.26	0.20	1.41 (1.25 to 1.58)	1.3×10^{-8}	99.8	99.3
rs11065756	First	0.34	0.21	1.92 (1.53 to 2.42)	1.2×10^{-8}	99.5	100
(Chr.12; 109823177)	Second	0.30	0.23	1.43 (1.20 to 1.71)	7.1×10^{-5}	100	100
	Third	0.27	0.22	1.26 (1.03 to 1.54)	0.026	100	99.9
	Combined	0.30	0.22	1.48 (1.33 to 1.66)	7.1×10^{-12}	99.9	100
rs11065783	First	0.40	0.30	1.56 (1.26 to 1.94)	4.9×10^{-5}	100	100
(Chr.12; 109880632)	Second	0.37	0.31	1.35 (1.14 to 1.59)	0.00046	100	100
	Third	0.33	0.28	1.24 (1.02 to 1.50)	0.029	99.7	100
	Combined	0.36	0.29	1.35 (1.21 to 1.50)	3.1×10^{-8}	99.9	100
rs12229654	First	0.34	0.21	1.99 (1.59 to 2.50)	2.1×10^{-9}	99.5	99.8
(Chr.12; 109898844)	Second	0.30	0.21	1.61 (1.35 to 1.93)	1.9×10^{-7}	100	100
	Third	0.27	0.20	1.54 (1.26 to 1.89)	3.4×10^{-5}	99.7	100
	Combined	0.30	0.20	1.66 (1.48 to 1.86)	3.3×10^{-18}	99.8	99.9
rs2074356	First	0.36	0.22	1.97 (1.57 to -2.46)	2.2×10^{-9}	100	100
(Chr.12; 111129784)	Second	0.32	0.23	1.53 (1.29 to 1.83)	1.7×10^{-6}	100	100
	Third	0.32	0.21	1.77 (1.46 to 2.16)	1.1×10^{-8}	100	100
	Combined	0.33	0.22	1.70 (1.52 to 1.90)	3.9×10^{-21}	100	100
rs11066280	First	0.40	0.26	1.92 (1.54 to 2.39)	3.2×10^{-9}	100	99.1
(Chr.12; 111302166)	Second	0.37	0.27	1.52 (1.29 to 1.81)	8.9×10^{-7}	100	100
	Third	0.36	0.25	1.71 (1.41 to 2.06)	2.8×10^{-8}	99.7	99.7
	Combined	0.37	0.26	1.68 (1.51 to 1.87)	2.5×10^{-21}	99.9	99.6

*SNP position is based on NCBI build 36.
†The number of samples at each stage was as follows: 209 and 1079 in the first stage, 479 and 863 in the second stage, and 365 and 780 in the third stage for OSCC and controls, respectively.
‡The odds ratio and p value were calculated by an allele test.

which reduce enzymatic activity (table 5). The frequency of the GG genotype of rs1229984 was higher in OSCC than in controls (0.20 vs. 0.06, OR=4.08, $p=4.4\times10^{-40}$). Similarly, the frequency of the AA+AG genotype of rs671 was higher in cases than in controls (0.73 vs 0.43, OR = 3.54, $p=5.5\times10^{-62}$). These results indicate that individuals who exhibit low enzymatic activity for *ADH1B* and/or *ALDH2* are at higher risk for OSCC.

Table 2 shows the ORs of OSCC associated with environmental and genetic risk factors along with their internal interactions. Ever-drinkers who did not smoke and ever-smokers who did not drink alcohol had significantly elevated adjusted ORs of 3.5 (95% CI 2.1 to 5.8) and 2.3 (95% CI 1.2 to 4.3), respectively. A supra-multiplicative OR of 16.0 (95% CI 9.7 to 26.3)—that is, statistically larger than the product of 3.5 and 2.3 (8.0), was found among individuals who were both ever-drinkers and ever-smokers. Subjects with only one risk allele, either rs671 AG/AA or rs1229984 GG, had significantly higher ORs of 4.8 (95% CI 3.7 to 6.3) and 3.1 (95% CI 1.6 to 6.1), respectively, than those without either risk allele. The OR for those with both genetic risk factors was 34.0 (95% CI 18.1 to 63.8); however, the interaction of these two genetic factors did not reach significance (p=0.079).

We also evaluated the combined effects of environmental and genetic risk factors (table 3). In this analysis, the reference group was composed of individuals who never drank or smoked and who also had no genetic risk factors. Compared with the reference group, ever-drinkers who did not smoke and had no genetic risk factors had a non-significant OR of 1.5 (95% CI 0.7 to 3.3). Non-drinkers and non-smokers with genetic risk factors also had a non-significant OR of 1.1 (95% CI 0.5 to 2.4). All other groups, however, had significantly elevated ORs. An interaction between alcohol drinking and smoking was observed only in the stratum with genetic risk. In the stratum with no genetic risk factors, alcohol drinking was not associated with OSCC, regardless of smoking status. Smoking without alcohol drinking elevated the ORs, regardless of the rs671 and rs1229984 genotypes, similarly and significantly. In contrast, interactions between alcohol drinking and genetic risk factors were highly significant. The combined effects of alcohol drinking and genetic risk factors were larger than the products of individual effects. For example, among non-smokers, the combined OR (12.1) was significantly larger than the product of the genetic effect (1.1) and the alcohol drinking risk (1.5). The same effect was seen among smokers ($62.1>1.1\times5.0$).

Finally, we evaluated the effect on OSCC of the number of risk factors present of the two possible environmental and two possible genetic factors (Figure 1). Compared with the no-risk-factor condition, the ORs for one, two, three and four risk factors were 1.4 (95% CI 0.7 to 2.7), 4.3 (95% CI 2.2 to 8.4), 41.0

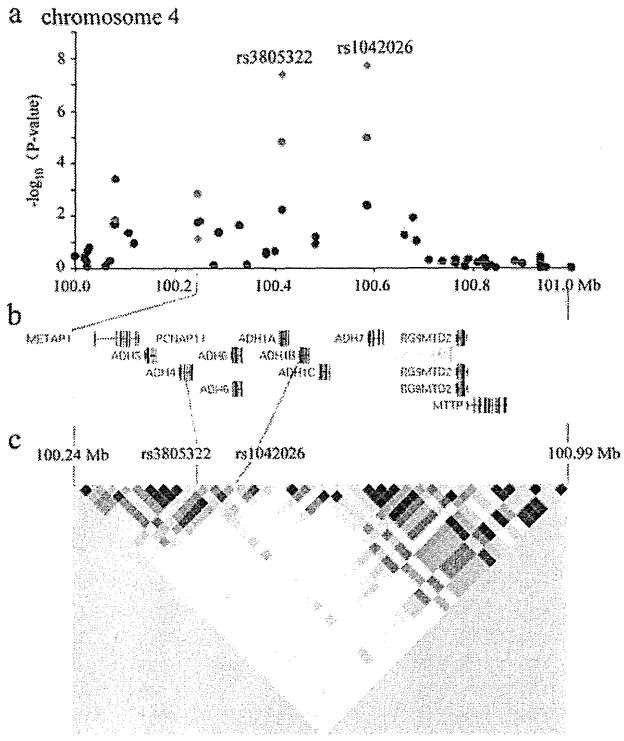

Figure 3 The 4q23 locus is associated with oesophageal squamous cell carcinoma (OSCC). (A) Single nucleotide polymorphism (SNP) single-marker association results. All genotyped SNPs at this locus in this study are plotted with their $-\log_{10}$(p value) for OSCC (allelic test) against chromosome position in Mb (100.0 to 101.0). Black, green and red dots indicate p values at the first, second and third screening stages. Two highly significant SNPs from the combined analysis, rs380532 and rs1042026, are shown. (B) The genomic location of RefSeq genes (100.24–100.99 Mb) with intron and exon structures is shown (UCSC Genome Browser on Human Mar. 2006 Assembly). (C) Pairwise square of the correlation coefficient (r^2) estimates for 39 SNPs from 100.24 Mb to 100.99 Mb in controls at the first stage, with increasing shades of grey indicating higher r^2 values.

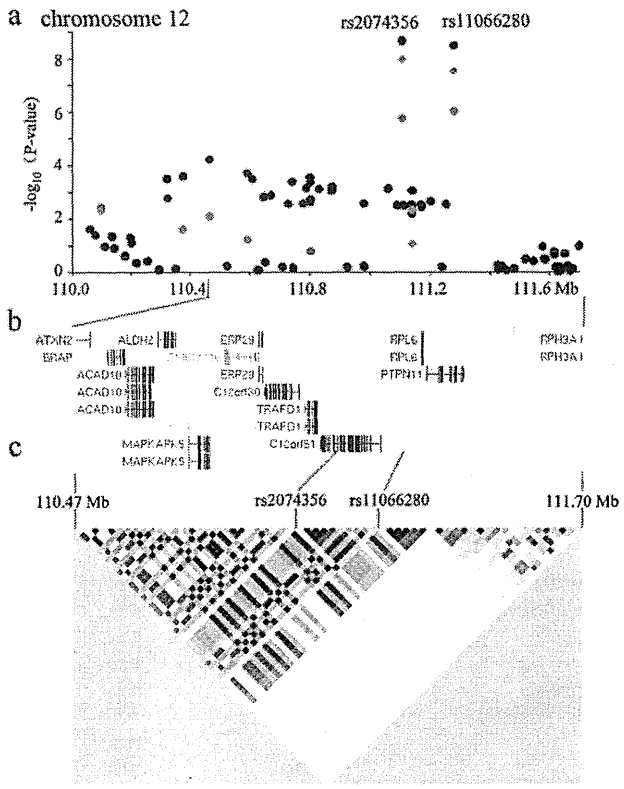

Figure 4 The 12q24.11-13 locus is associated with oesophageal squamous cell carcinoma (OSCC). (A) Single nucleotide polymorphism (SNP) single-marker association results. All SNPs genotyped at this locus in this study are plotted with their $-\log_{10}$(p value) for OSCC (allelic test) against chromosome position in Mb (110.0–111.7). Black, green and red dots indicate p values at the first, second and third screening stages. Two highly significant SNPs in the combined analysis, rs2074356 and rs11066280, are shown. (B) The genomic location of RefSeq genes (110.47–111.70 Mb) with intron and exon structure is shown (UCSC Genome Browser on Human Mar. 2006 Assembly). (C) Pairwise square of the correlation coefficient (r^2) estimates for 63 SNPs from 110.47 Mb to 111.70 Mb in controls at the first stage, with increasing shades of grey indicating higher r^2 values.

(95% CI 20.2 to 83.3) and 357.1 (95% CI 105.4 to 1209.5), respectively. A highly significant linear trend ($p<0.0001$) was observed.

DISCUSSION

Individuals who smoke and drink alcohol are considered at high risk for OSCC, although most such people do not develop the disease. Indeed, in a recent study, only 41 of 100 000 such people developed OSCC.[9] Therefore, it is crucial to simultaneously analyse genetic and environmental risk factors to more efficiently identify people at truly high risk for OSCC. This unbiased genome-wide association study identified two loci

Table 5 Association of non-synonymous single nucleotide polymorphisms (SNPs) in *ADH1B* and *ALDH2* with oesophageal squamous cell carcinoma (OSCC)

SNP (Chromosome; gene)	Study group*	Genotype frequency†			Allele frequency		HWE test p Value	Genotype association test‡ OR (95% CI)	p Value	Allele association test OR (95% CI)	p Value	PAR§ (%)
		GG	GA	AA	G	A						
rs1229984	OSCC	0.20	0.32	0.48	0.36	0.64	9.4×10^{-23}	4.08 (3.27 to 5.09)	4.4×10^{-40}	1.82 (1.63 to 2.03)	6.23×10^{-28}	41.5
(Chr.4; *ADH1B*)	Control	0.06	0.35	0.59	0.23	0.77	0.56					
		AA	AG	GG	A	G						
rs671	OSCC	0.01	0.72	0.27	0.37	0.63	1.7×10^{-81}	3.54 (3.04 to 4.14)	5.5×10^{-62}	1.78 (1.60 to 1.98)	1.03×10^{-26}	38.8
(Chr.12; *ALDH2*)	Control	0.07	0.36	0.57	0.25	0.75	0.12					

The risk allele of rs1229984 (G) and rs671 (A) encode arginine at position 48 and lysine at position 504, respectively, which are known to reduce enzymatic activity.
HWE, Hardy–Weinberg equilibrium.
*The number of OSCC and control samples was 1071 and 2762, respectively.
†The genotyping success rate of rs1229984 and rs671 was 99.84% and 99.79%, respectively.
‡A genotype association analysis was performed for GG versus GA+AA genotype in rs1229984 and for AA+AG versus GG genotype in rs671.
§The population attributable risk (PAR = AF*(OR − 1)/(AF*(OR − 1) + 1)) (AF, allele frequency) is defined as the reduction in the incidence of the disease if the population were not exposed to the risk allele.

containing genes involved in alcohol metabolism. In addition, we found a strong genetic-environmental interaction related to the risk of OSCC. Subjects with two environmental risk factors (ever-smokers and ever-drinkers) in combination with two genetic risk factors (AA or GA at rs1229984 (*ADH1B*) and GG at rs671 (*ALDH2*)) had a much higher risk than other subjects. Specifically, compared with no risk factor, the ORs with one, two, three and four risk factors were 1.4 (95% CI 0.7 to 2.7), 4.3 (95% CI 2.2 to 8.4), 41.0 (95% CI 20.2 to 83.3), and 357.1 (95% CI 105.4 to 1209.5), respectively. Of all of the risk factors for OSCC that we had previously examined, the combination of all four factors studied had the highest risk, with an OR of 357.1.

This information on the strong genetic-environmental interaction is valuable for secondary prevention of OSCC. When we see subjects who show *ADH1B* (rs1229984) and *ALDH2* (rs671) variants as well as smoking and drinking habits, we will advise them to have a periodic upper gastrointestinal fibre test. Screening of these patients could have an important role in the early detection of OSCC. Furthermore, the information gained from this study may also enable the development of a primary individualised prevention strategy for young people with these genetic variations. When subjects have these high-risk variants, advising them not to start smoking or, especially, not to drink alcohol will dramatically reduce their risk of developing OSCC. We observed that drinkers who consumed alcohol daily and heavy smokers had higher ORs than their counterparts, and the ORs decreased with an increased amount of time since quitting these habits. However, all ORs among ever-drinkers/smokers were significantly higher than 1.0 (supplementary table 2). At present, we cannot unequivocally determine the preventive effect of quitting smoking or drinking alcohol. To determine whether stopping these habits reduces the risk of OSCC, prospective studies are needed.

Several limitations of this study should be mentioned. First, the statistical power of this genome-wide association study was not sufficient for allelic variants with an OR of <1.5 (supplementary table 1). Therefore, we might have missed variants with a small effect size (eg, 1.1–1.3), which are often reported for other life-style-related diseases. Second, we did not match the cases and controls; thus, the basic distributions of sex, place of residence and age were different between the two groups (table 1). However, although matching is efficient in data collection, it does not affect the point estimation if the factor is included in the model. Thus, the absence of matching did not distort the results. Third, personalised genetic testing is prohibitively expensive and ethically problematic. Finally, because of the retrospective study design, several answers in the questionnaire could be altered by disease or pre-disease conditions. Thus, the high OR among former drinkers and smokers who had quit less than 1 year previously may incorrectly imply a causal relationship between these habits and OSCC risk. Therefore, the effect of quitting these habits on OSCC risk should be examined by prospective studies.

Hashibe *et al* identified the variation of *ADH1B* (rs1229984) as a risk factor for OSCC.[10] They conducted their analysis on European and Latin American populations, and the result was consistent with the results of our study of Japanese patients and controls. A study of Chinese people also demonstrated that *ADH1B* (rs1229984) is a risk factor for OSCC.[11] Recently, Cui *et al* reported that variations of *ADH1B* (rs1229984) and *ALDH2* (rs671) coupled with alcohol drinking and smoking synergistically enhance oesophageal cancer risk.[12] Their study indicates that these two genetic risk variants provide almost equal risk for the generation of OSCC. In our study, among individuals without a genetic risk, alcohol consumption did not increase the OR of OSCC significantly. For people without genetic risk, smoking habits were the major contributing factor for the generation of OSCC. However, in people with genetic risk, a drinking habit strikingly increased the risk of OSCC; combined with smoking, it increased the risk even further (table 3).

Smoking- and alcohol drinking-related genes such as the *ADH* family, the *ALDH* family and nicotinic acetylcholine receptors, especially as indicated in SNP analyses, have been significantly associated with a variety of cancers[10 13–15] We performed an association analysis between OSCC and SNPs in the nicotinic acetylcholine receptor subunit genes *CHRNA3* and *CHRNA5* at 15q25 using the same cases and controls. An association with lung cancer was reported by Hung *et al*[14] and Thorgeirsson et *al*[13] However, in this study, we did not find a significant association at either rs1051730 (*CHRNA3*) or rs16969968 (*CHRNA5*), with ORs of 0.91 and 0.89, respectively (supplementary table 3). Smoking habits contributed to the development of OSCC; however, SNPs other than rs1051730 (*CHRNA3*) or rs16969968 (*CHRNA5*) might affect OSCC generation. Because the risk allele frequency of both of these SNPs was <0.02 in cases and controls in this study population, it would be difficult to show any difference between cases and controls. Variants of *ECRG1* have been reported to be associated with OSCC.[16] However, it is still unclear whether the genetic or epigenetic changes caused by smoking and/or alcohol drinking are directly associated with the development of OSCC in cooperation with SNPs of genes such as those of the ADH family, the ALDH family and nicotinic acetylcholine receptors[5 17] ADH1B in subjects with the rs1229984 AA or GA genotype is reported to metabolise ethanol up to 40 times more quickly than ADH1B from GG homozygotes.[18] Furthermore, ALDH2 from subjects with the GG allele of rs671 is reported to metabolise acetaldehyde more than 100 times faster than from AG ALDH2 heterozygotes.[19] In addition, *ADH* genes exhibit a nominally significant association with smoking behaviour.[20] Considering our results and these reports, higher local exposure to ethanol and acetaldehyde mediated by smoking may be strongly associated with OSCC development. To answer these questions, it is necessary to conduct a prospective study in genetically at-risk populations with or without drinking and/or smoking habits, as recently performed for type 2 diabetes.[21 22]

In summary, this study disclosed a significant genetic-environmental interaction, with very large ORs, associated with the development of OSCC. Thus, convincing young people to smoke and drink less is likely to reduce the incidence of OSCC. SNP genotyping demonstrated that the *ADH1B* and/or *ALDH2* risk alleles had an interaction with smoking and, especially, alcohol consumption. Analysis of *ADH1B* and *ALDH2* variants would be valuable for secondary prevention of OSCC in high-risk patients who smoke and drink alcohol. Our findings, if replicated in other groups, could demonstrate new pathophysiological pathways for the development of OSCC.

Acknowledgements We thank Ms. Judith Clayton for her critical reading of the manuscript.

Funding This work was supported in part by the following grants and foundations: Japan Society for the Promotion of Science (JSPS) Grant-in-Aid for Scientific Research, grant numbers 17109013, 21229015; CREST, Japan Science and Technology Agency (JST); NEDO (New Energy and Industrial Technology Development Organization) Technological Development for Chromosome Analysis; and The Ministry of Education, Culture, Sports, Science, and Technology of Japan for Scientific Research on Priority Areas, Cancer Translational Research Project, Japan. Other Funders: Japan Society for the Promotion of Science (JSPS) Grant-in-Aid for Scientific Research, Japan Science and Technology Agency, New Energy and Industrial Technology Development Organization.

Competing interests None.

Ethics approval This study was conducted with the approval of the Kyusyu University, Juntendo University, National Cancer Institute, Saitama Cancer Center, Kurume University, and Kurume University, Japan.

Contributors KY, SS, and H Inoue equally contributed to this study. FT, KY, MT, HK, HF, YT, SN, ST, KM, KI, ST, NH, H Ishii, H Inoue and MM jointly designed the study and organised the recruitment of participants. Y Kajiyama, H Igaki, KF, TT, Y Kawashima, and TS organised the recruitment of participants and biological samples. KY conducted the SNP study and the statistical analysis and drafted the manuscript. SS organised the environmental study and the statistical analysis and drafted the manuscript. FT had full access to all of the data in the study and takes responsibility for the integrity of the data and the accuracy of the data analysis.

Provenance and peer review Not commissioned; externally peer reviewed.

REFERENCES

1. **Shimada H,** Kitabayashi H, Nabeya Y, *et al*. Treatment response and prognosis of patients after recurrence of esophageal cancer. *Surgery* 2003;**133**:24–31.
2. **Parkin DM,** Bray F, Ferlay J, *et al*. Global cancer statistics, 2002. *CA Cancer J Clin* 2005;**55**:74–108.
3. **Brooks PJ,** Enoch MA, Goldman D, *et al*. The alcohol flushing response: an unrecognized risk factor for esophageal cancer from alcohol consumption. *PLoS Med* 2009;**6**:e50.
4. **Tsuchihashi-Makaya M,** Serizawa M, Yanai K, *et al*. Gene-environmental interaction regarding alcohol-metabolizing enzymes in the Japanese general population. *Hypertens Res* 2009;**32**:207–13.
5. **Druesne-Pecollo N,** Tehard B, Mallet Y, *et al*. Alcohol and genetic polymorphisms: effect on risk of alcohol-related cancer. *Lancet Oncol* 2009;**10**:173–80.
6. **Purcell S,** Neale B, Todd-Brown K, *et al*. PLINK: a tool set for whole-genome association and population-based linkage analyses. *Am J Hum Genet* 2007;**81**:559–75.
7. **Barrett JC,** Fry B, Maller J, *et al*. Haploview: analysis and visualization of LD and haplotype maps. *Bioinformatics* 2005;**21**:263–5.
8. **Dupont WD,** Plummer WD Jr. Power and sample size calculations. A review and computer program. *Control Clin Trials* 1990;**11**:116–28.
9. **Ishiguro S,** Sasazuki S, Inoue M, *et al*. Effect of alcohol consumption, cigarette smoking and flushing response on esophageal cancer risk: a population-based cohort study (JPHC study). *Cancer Lett* 2009;**275**:240–6.
10. **Hashibe M,** McKay JD, Curado MP, *et al*. Multiple ADH genes are associated with upper aerodigestive cancers. *Nat Genet* 2008;**40**:707–9.
11. **Yang SJ,** Wang HY, Li XQ, *et al*. Genetic polymorphisms of ADH2 and ALDH2 association with esophageal cancer risk in southwest China. *World J Gastroenterol* 2007;**13**:5760–4.
12. **Cui R,** Kamatani Y, Takahashi A, *et al*. Functional variants in ADH1B and ALDH2 coupled with alcohol and smoking synergistically enhance esophageal cancer risk. *Gastroenterology* 2009;**137**:1768–75.
13. **Thorgeirsson TE,** Geller F, Sulem P, *et al*. A variant associated with nicotine dependence, lung cancer and peripheral arterial disease. *Nature* 2008;**452**:638–42.
14. **Hung RJ,** McKay JD, Gaborieau V, *et al*. A susceptibility locus for lung cancer maps to nicotinic acetylcholine receptor subunit genes on 15q25. *Nature* 2008;**452**:633–7.
15. **Berrettini W,** Yuan X, Tozzi F, *et al*. Alpha-5/alpha-3 nicotinic receptor subunit alleles increase risk for heavy smoking. *Mol Psychiatry* 2008;**13**:368–73.
16. **Li Y,** Zhang X, Huang G, *et al*. Identification of a novel polymorphism Arg290Gln of esophageal cancer related gene 1 (ECRG1) and its related risk to esophageal squamous cell carcinoma. *Carcinogenesis* 2006;**27**:798–802.
17. **Chanock SJ,** Hunter DJ. Genomics: when the smoke clears. *Nature* 2008;**452**:537–8.
18. **Hashibe M,** Boffetta P, Zaridze D, *et al*. Evidence for an important role of alcohol- and aldehyde-metabolizing genes in cancers of the upper aerodigestive tract. *Cancer Epidemiol Biomarkers Prev* 2006;**15**:696–703.
19. **Peng GS,** Yin SJ. Effect of the allelic variants of aldehyde dehydrogenase ALDH2*2 and alcohol dehydrogenase ADH1B*2 on blood acetaldehyde concentrations. *Hum Genomics* 2009;**3**:121–7.
20. **Caporaso N,** Gu F, Chatterjee N, *et al*. Genome-wide and candidate gene association study of cigarette smoking behaviors. *PLoS ONE* 2009;**4**:e4653.
21. **Meigs JB,** Shrader P, Sullivan LM, *et al*. Genotype score in addition to common risk factors for prediction of type 2 diabetes. *N Engl J Med* 2008;**359**:2208–19.
22. **Lyssenko V,** Jonsson A, Almgren P, *et al*. Clinical risk factors, DNA variants, and the development of type 2 diabetes. *N Engl J Med* 2008;**359**:2220–32.

Editor's quiz: GI snapshot

Pizza, beer, amylase, lipase and the acute abdomen

CLINICAL PRESENTATION

A previously healthy 16-year-old male student was admitted with acute abdominal pain after eating two large pizzas and drinking five pints (approximately 2.8 l) of beer (alcohol content 4.5%). Initial assessment revealed epigastric tenderness with elevated serum amylase (380 IU/l, normal 30–110 IU/l) and lipase (4398 IU/l, normal 23–300 IU/l) concentrations. There was no free gas on the chest radiograph. The patient developed increasing abdominal pain, tenderness, tachycardia and a lactic acidosis (pH 7.20, lactate 2.91 mmol/l) within 6 h. Contrast-enhanced abdominal CT (figure 1) was done 8 h after admission.

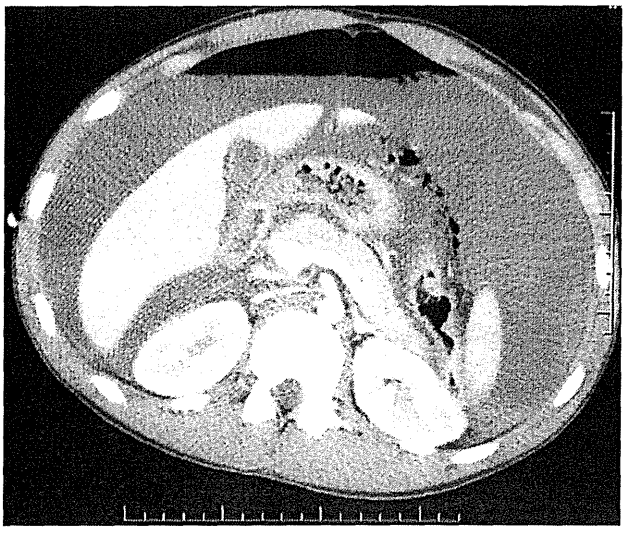

Figure 1 Contrast-enhanced CT scan of the abdomen.

QUESTION

What are the findings on CT?

See page 1560 for answer

James A Catton, Dileep N Lobo

Division of Gastrointestinal Surgery, Nottingham Digestive Diseases Centre NIHR Biomedical Research Unit, Nottingham University Hospitals, Queen's Medical Centre, Nottingham, UK

Correspondence to Mr D.N. Lobo, Division of Gastrointestinal Surgery, E Floor, West Block, Nottingham University Hospitals, Queen's Medical Centre, Nottingham NG7 2UH, UK; dileep.lobo@nottingham.ac.uk

Competing interests None.

Patient consent Obtained from parent.

Provenance and peer review Not commissioned; not externally peer reviewed.

Gut 2010;**59**:1464. doi:10.1136/gut.2009.184010

GASTROENTEROLOGY 2010;138:1312–1320

Effects of Ghrelin Administration After Total Gastrectomy: A Prospective, Randomized, Placebo-Controlled Phase II Study

SHINICHI ADACHI,* SHUJI TAKIGUCHI,* KAZUYUKI OKADA,‡ KAZUYOSHI YAMAMOTO,* MAKOTO YAMASAKI,* HIROSHI MIYATA,* KIYOKAZU NAKAJIMA,* YOSHIYUKI FUJIWARA,* HIROSHI HOSODA,§ KENJI KANGAWA,§ MASAKI MORI,* and YUICHIRO DOKI*

*Department of Gastroenterological Surgery, Osaka University Graduate School of Medicine, Osaka; ‡Department of Surgery, Suita Municipal Hospital, Osaka; and §Department of Biochemistry, National Cardiovascular Center Research Institute, Osaka, Japan

BACKGROUND & AIMS: Body weight (BW) loss and reduction of blood ghrelin level are commonly observed after total gastrectomy (TG). A prospective study was designed to elucidate whether exogenous ghrelin administration prevents postoperative BW loss by improving appetite and oral food intake in patients with gastric cancer after undergoing TG. **METHODS:** In this randomized phase II study, 21 patients undergoing TG were assigned to a ghrelin (11 patients) or placebo group (10 patients). They received intravenous infusion of synthetic human ghrelin (3 μg/kg) or saline twice daily for 10 days after starting oral food intake following surgery. Changes in BW, appetite visual analog scale score, food intake calories, body composition, basal metabolic rate, and various blood test results were evaluated. **RESULTS:** Excluding one patient who developed profound diaphoresis during ghrelin infusion, 20 patients completed the study. Food intake and appetite were significantly higher with ghrelin compared with placebo (average, 13.8 vs 10.4 kcal/kg/day [$P = .030$] and 5.7 vs 3.9 cm [$P = .032$], respectively). BW loss was significantly lower in the ghrelin than in the placebo group (−1.4% vs −3.7%; $P = .044$). Fat mass, lean body mass, and basal metabolic rate decreased significantly in the placebo group; however, the reductions in lean body mass and basal metabolic rate were not significant in the ghrelin group, although that of fat mass was significant. **CONCLUSIONS: Short-term administration of synthetic ghrelin was safe and successfully lessened postoperative BW loss and improved appetite and food intake after TG.**

Keywords: Ghrelin; Total Gastrectomy; Gastric Cancer; Body Weight Loss.

Body weight loss is common and a serious outcome in patients with gastric cancer who have undergone total gastrectomy. It correlates well with decline in postoperative quality of life and is the most reliable indicator of malnutrition, which impairs immune function, infection susceptibility, and survival.[1–3] Although various mechanisms have been considered, such as perturbation of absorption due to reduced pancreatic excretion,[4,5] decrease of gastric acid level,[6] reflux esophagitis,[7] intestinal floral alteration,[8] and increased peristalsis and diarrhea,[9] reduced food intake[10,11] is the most conceivable explanation for body weight loss after total gastrectomy. Therefore, surgeons dealing with gastric cancers have tried to increase food intake by producing a gastric substitute, such as a jejunal pouch, but such procedures have not always been successful.[12] Another study indicated that the majority of patients with total gastrectomy could eat food as much as healthy subjects under a regulated program.[13] Our own experience indicates that some patients do not show significant body weight loss after total gastrectomy by resorting to small but frequent meals. These changes suggest that reduced food intake after total gastrectomy could not be simply explained by loss of storage volume due to gastrectomy, but rather reflect a disturbance of eating activity through an unknown mechanism.

The 28-amino acid peptide ghrelin is the endogenous ligand for the growth hormone (GH) secretagogue receptor 1a, which stimulates GH release from the pituitary gland.[14] The majority of ghrelin is produced by X/A-like cells of the oxyntic glands in the stomach, and a smaller amount is secreted from other organs, such as the intestine, pancreas, kidney, and hypothalamus.[15,16] Ghrelin has various physiologic functions in addition to secretion of GH, such as promoting the appetite signal in the hypothalamus (in contrast to leptin),[17] stimulating gastrointestinal activity (such as peristalsis, gastric acid secretion, and pancreatic excretion through the vagal nerves),[18] and regulation of fat metabolism.[19] In addition, ghrelin mitigates proinflammatory cytokine production and attenuates the stress signal.[20] Among the pleiotropic functions of ghrelin, this peptide is the only gastrointestinal hormone known to stimulate appetite. A randomized double-blind study of healthy volunteers

Abbreviations used in this paper: ANOVA, analysis of variance; BMR, body metabolic rate; GH, growth hormone; IGF, insulin-like growth factor.

0016-5085/10/$36.00
doi:10.1053/j.gastro.2009.12.058